A Capability for Severe Weather Automated/Assisted Ship Handling (SWASH)

Dick K. P. Yue
Department of Ocean Engineering
MIT

Workshop on Free Surface Water Waves

The Fields Institute for Research in Mathematical Sciences
Toronto, Canada

June 14-18, 2004

Motivation:

- Recent advances in wave sensing, nonlinear wave modeling, and high performance computing, have made it possible to perform large-scale phase-resolved simulations of nonlinear wave-fields to obtain practically useful deterministic reconstruction and forecasting.

Objective/Applications:

- Provide framework for assimilation, integration and optimal deployment of wave sensing systems.
- Direct phase-resolved deterministic prediction of wave-field evolution.
- Automated steering and deterministic path planning of manned and unmanned surface vehicles to achieve "severe weather automated/assisted ship handling" (SWASH).

Focus of the SWASH Concept: Multi-Level Control

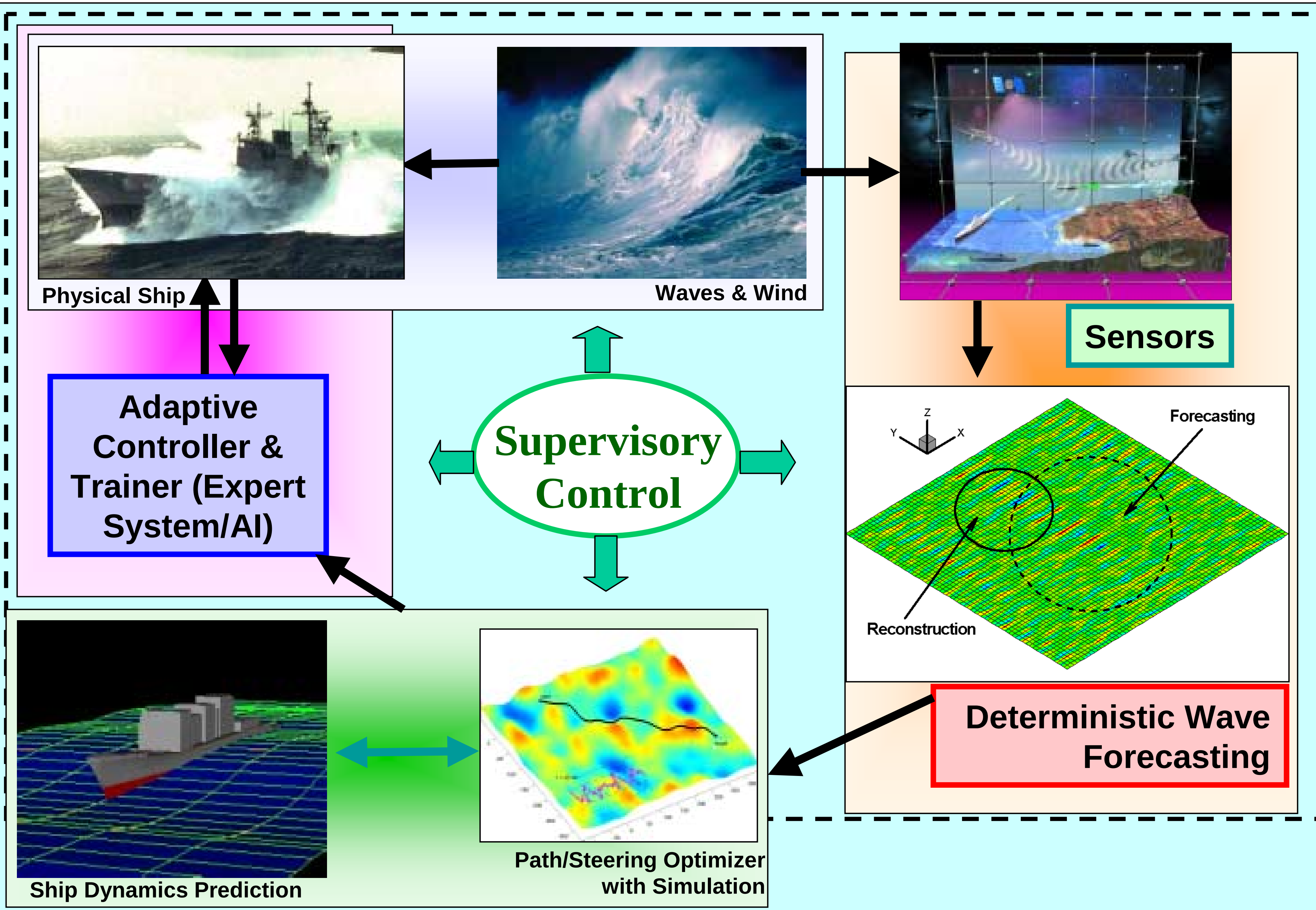

Approach

- Extend high-order spectral (HOS) method (mode coupling approach using arbitrary large number of modes N and nonlinearity order M; exponential convergence and almost linear computational effort with M and N) for simulation of ocean wave-field evolution to include:
  - finite depth and variable bottom topography
  - variable ambient current
  - dissipation due to wave breaking
  - so far not modeled: wind forcing, bottom friction and viscous effects
- Reconstruct nonlinear ocean wave-field using multi-level optimization scheme
  - arbitrary order of nonlinearity
  - scalability for high performance computing
  - straightforward extension to multiple hybrid wave measurement data
- Implement HOS wave model on high performance computing platforms for large-scale simulations
  - $L^2 \sim O(10^{3\text{-}4}\ \text{km}^2)$, $T \sim O(10^{3\text{-}4}\ \text{sec.})$; $(N \sim O(10^{6\text{-}8})$; $M \sim O(3\text{-}5))$.

Comparison to Exact Stokes Waves
(Dommermuth & Yue 1987)

Maximum absolute error in vertical surface velocity:

ε	N	M= 2	4	6	8	10	12	14
.1	8	$.75\times10^{-3}$	$.68\times10^{-5}$	$.72\times10^{-7}$	$.22\times10^{-8}$	$.10\times10^{-8}$		
	16	$.75\times10^{-3}$	$.68\times10^{-5}$	$.65\times10^{-7}$	$.64\times10^{-9}$	$.49\times10^{-10}$		
.2	8	$.59\times10^{-2}$	$.22\times10^{-3}$	$.15\times10^{-4}$	$.18\times10^{-5}$	$.13\times10^{-5}$		
	16	$.60\times10^{-2}$	$.22\times10^{-3}$	$.87\times10^{-5}$	$.37\times10^{-6}$	$.38\times10^{-7}$		
	32	$.60\times10^{-2}$	$.22\times10^{-3}$	$.88\times10^{-5}$	$.35\times10^{-6}$	$.14\times10^{-7}$	$.75\times10^{-9}$	
.3	8	$.19\times10^{-1}$	$.22\times10^{-2}$	$.47\times10^{-3}$	$.14\times10^{-3}$	$.16\times10^{-3}$		
	16	$.20\times10^{-1}$	$.18\times10^{-2}$	$.19\times10^{-3}$	$.59\times10^{-4}$	$.24\times10^{-4}$		
	32	$.20\times10^{-1}$	$.18\times10^{-2}$	$.17\times10^{-3}$	$.16\times10^{-4}$	$.17\times10^{-5}$		
	64	$.20\times10^{-1}$	$.18\times10^{-2}$	$.17\times10^{-3}$	$.16\times10^{-4}$	$.16\times10^{-5}$	$.21\times10^{-6}$	$.33\times10^{-7}$
.35	8	$.31\times10^{-1}$	$.64\times10^{-2}$	$.22\times10^{-2}$	$.13\times10^{-2}$	$.13\times10^{-2}$		
	16	$.31\times10^{-1}$	$.41\times10^{-2}$	$.99\times10^{-3}$	$.71\times10^{-3}$	$.22\times10^{-3}$		
	32	$.31\times10^{-1}$	$.40\times10^{-2}$	$.53\times10^{-3}$	$.94\times10^{-4}$	$.95\times10^{-4}$	$.16\times10^{-3}$	
	64	$.31\times10^{-1}$	$.40\times10^{-2}$	$.53\times10^{-3}$	$.73\times10^{-4}$	$.11\times10^{-4}$	$.38\times10^{-5}$	$.68\times10^{-3}$
.40	32	$.45\times10^{-1}$	$.79\times10^{-2}$	$.28\times10^{-2}$	$.81\times10^{-2}$			
	4	$.45\times10^{-1}$	$.79\times10^{-2}$	$.15\times10^{-2}$	$.35\times10^{-3}$	$.91\times10^{-3}$		
	28	$.45\times10^{-1}$	$.79\times10^{-2}$	$.15\times10^{-2}$	$.30\times10^{-3}$	$.89\times10^{-3}$		

- **Exponential Convergence with N & M**

Long-Time Evolution of Nonlinear Wavetrain (Dommermuth & Yue 1987)

Steepening Stokes wave:

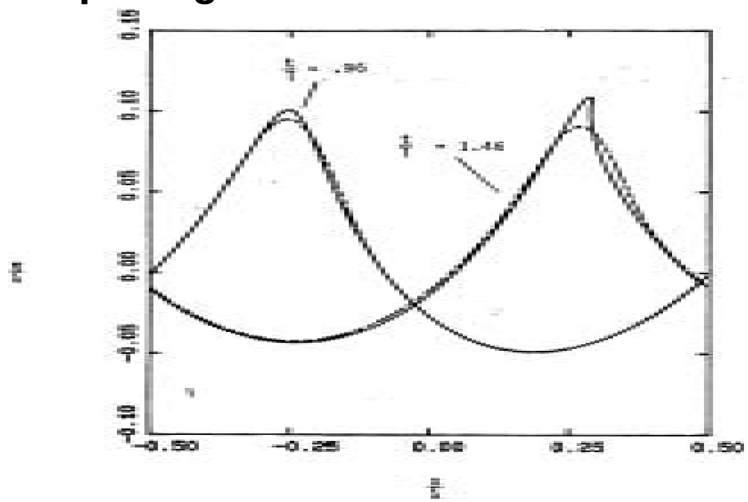

Energy dissipation due to wave breaking:

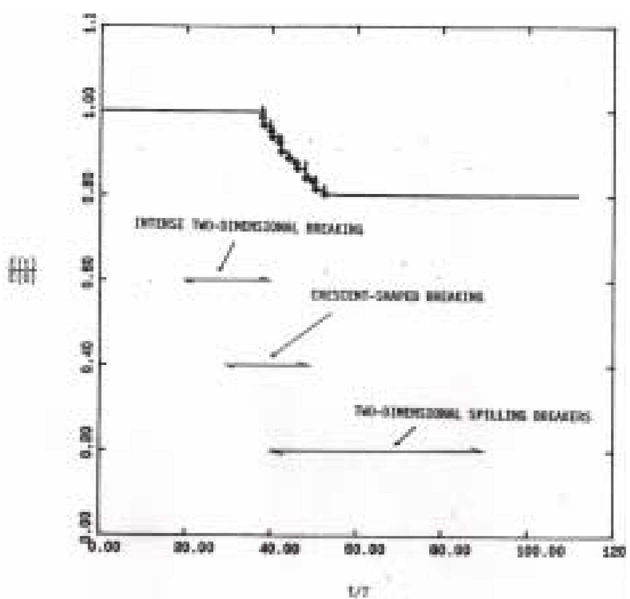

Steepening/breaking wave packet:

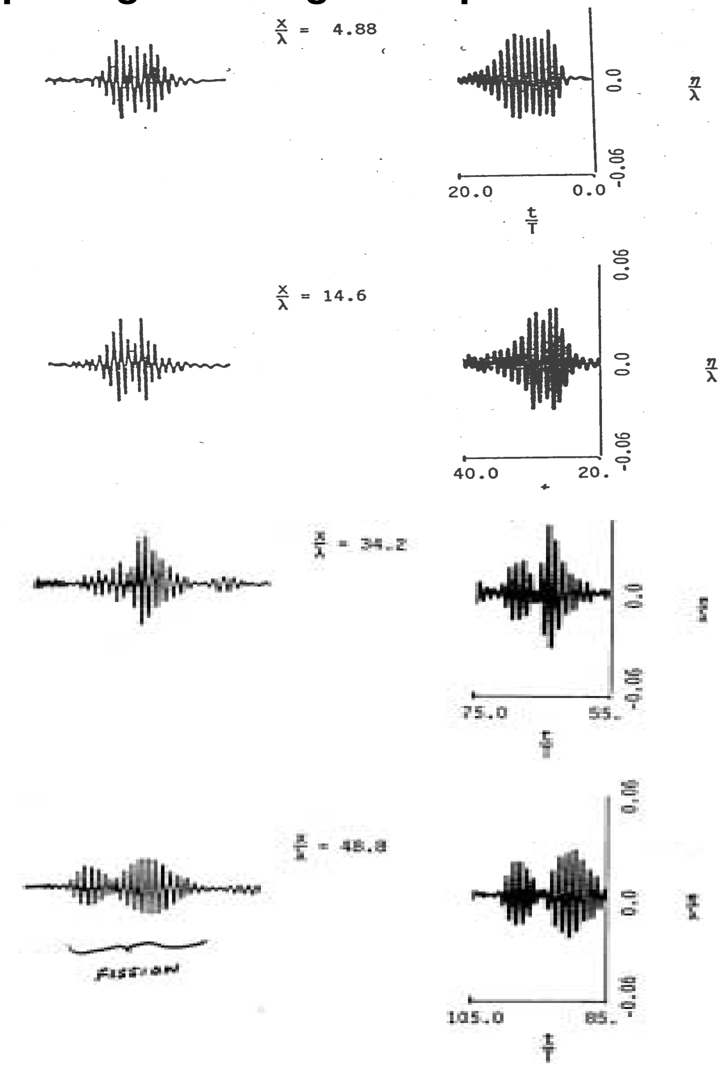

Experiment (Su 1982) **Simulation**

Comparison with Experiment—Wave Breaking

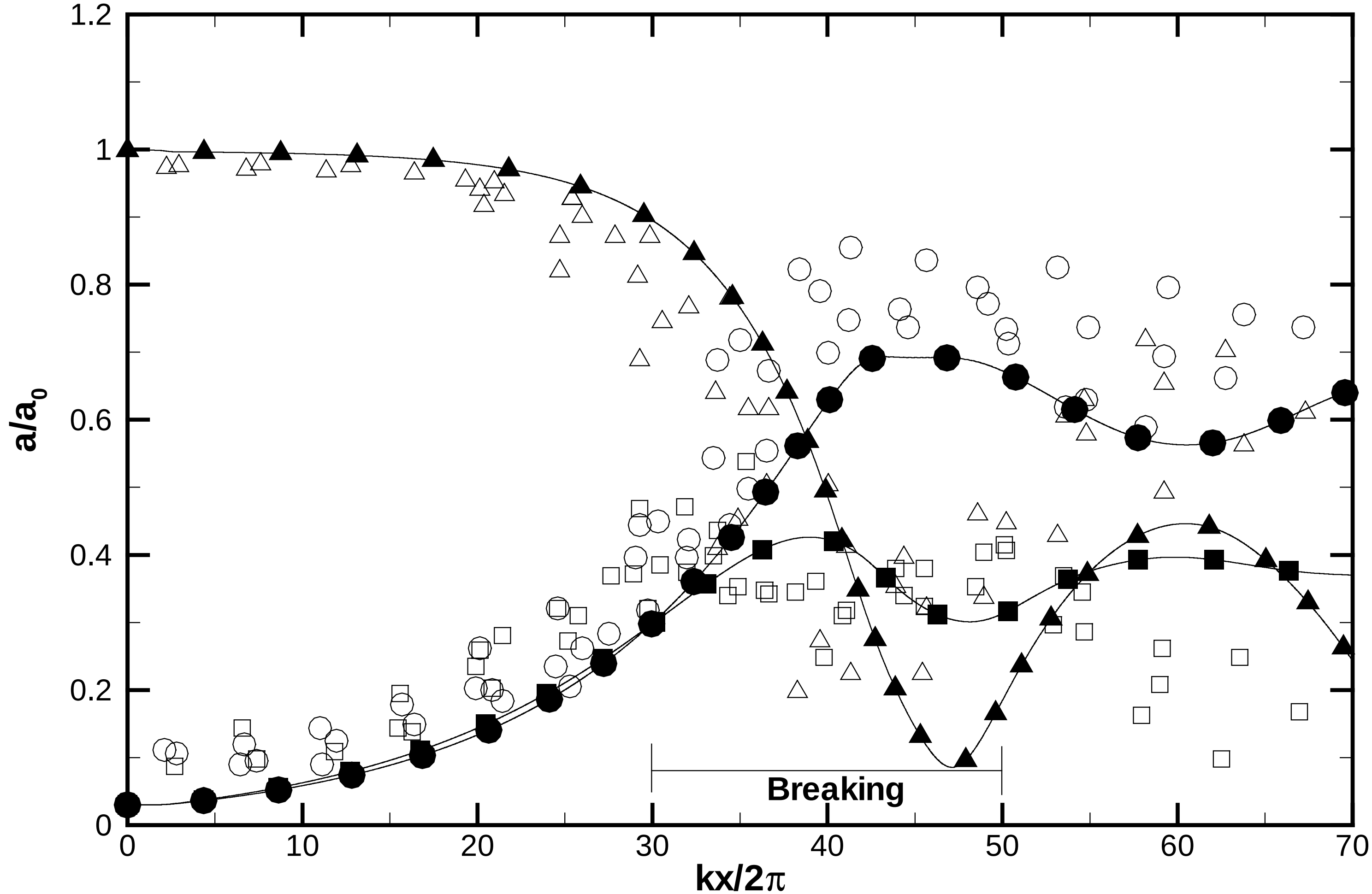

	HOS (M=5)	Experiments (Tulin & Waseda 1999)
carrier wave	▲	Δ
lower side band	●	○
upper sideband	■	□

Nonlinear Wave-Bottom Interaction (Liu & Yue 1998)

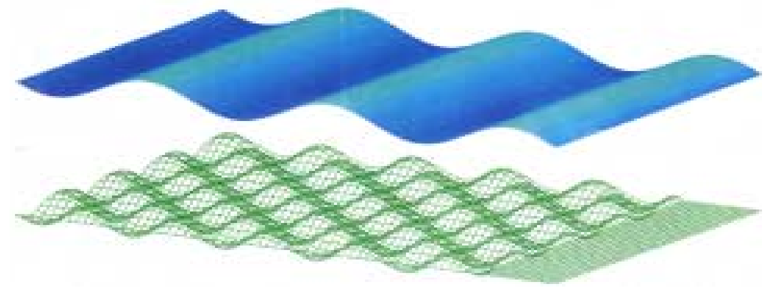

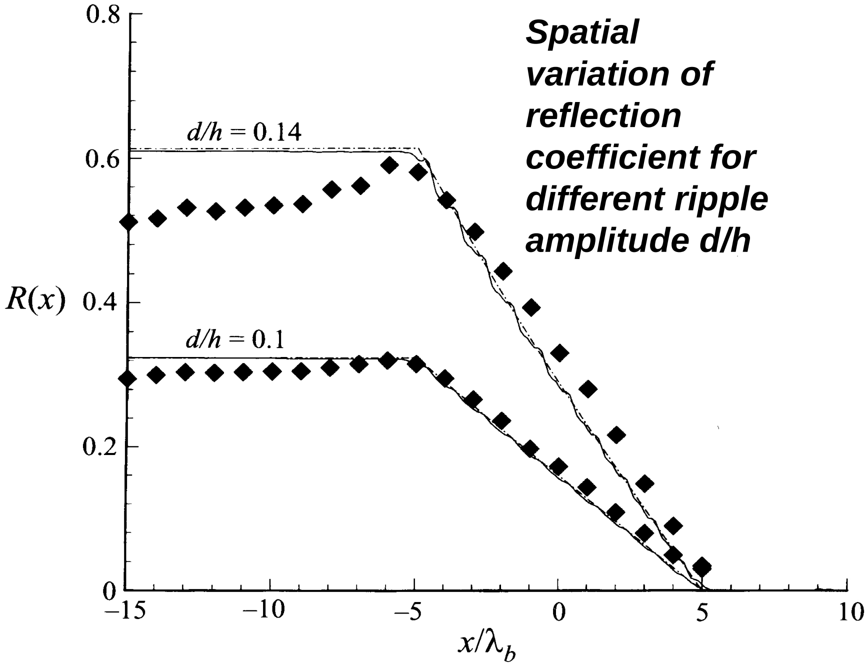

Spatial variation of reflection coefficient for different ripple amplitude d/h

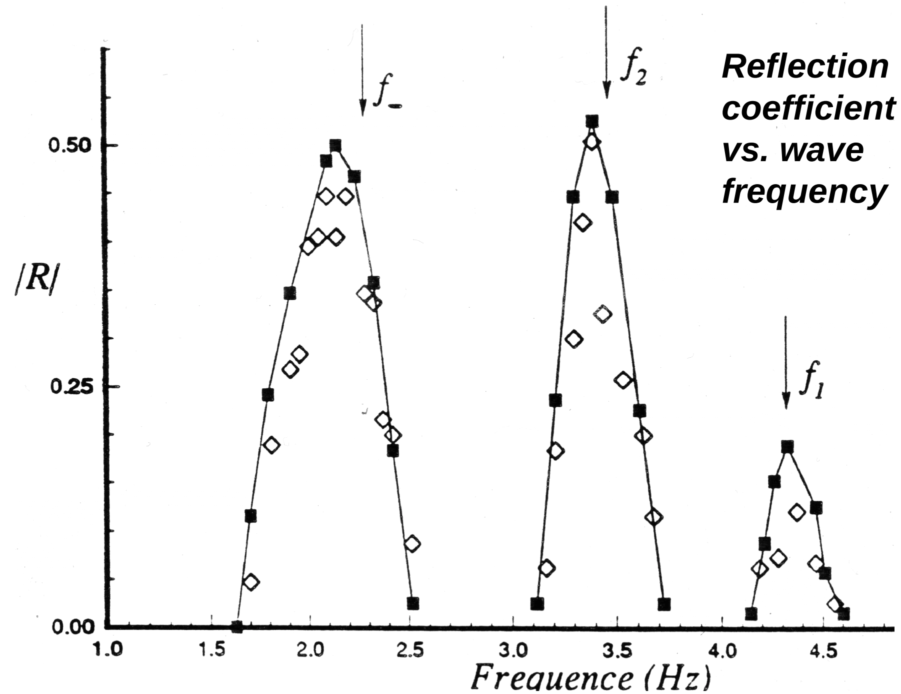

Reflection coefficient vs. wave frequency

Experiment (◆, ◊); HOS (——)

- ➢Waves traveling over near-shore variable bottom topography may result in strong nonlinear wave-bottom interactions
- ➢Distinctive forward and reflected (Bragg-like) wave signatures associated with characteristics of wave-field and bottom topography

Nonlinear Wave Reflection in Opposing Variable Current

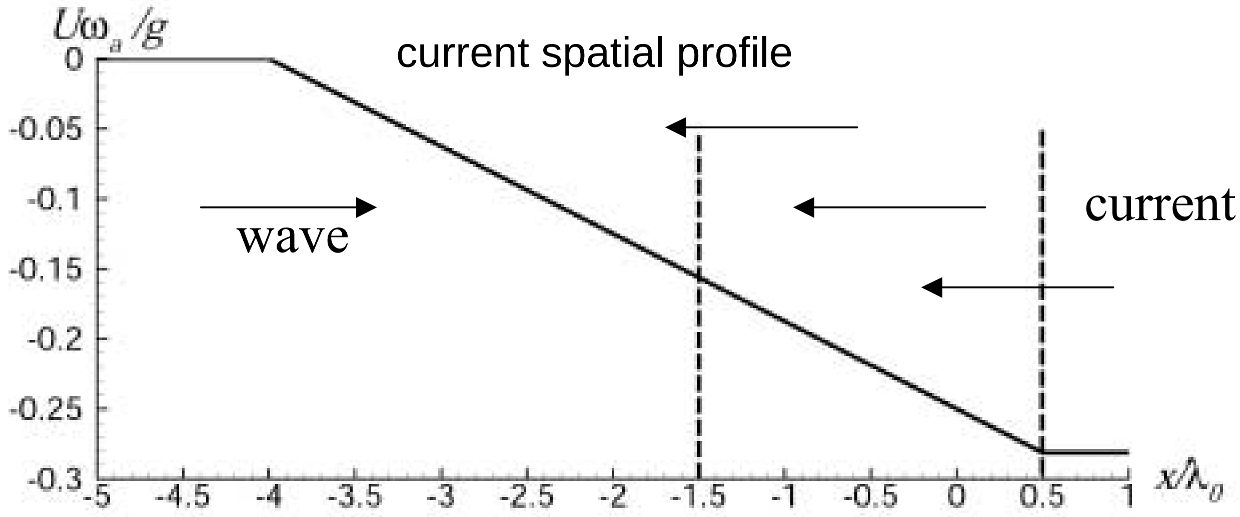

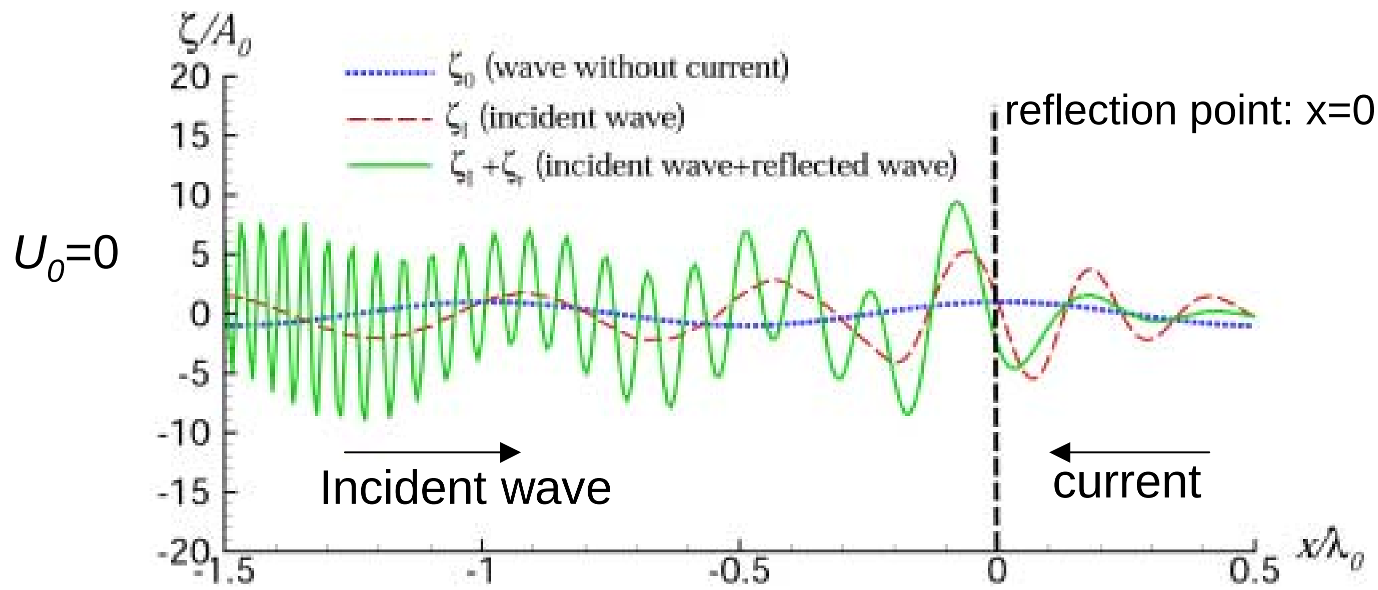

wave elevation in space

Comparison of Linear and Nonlinear Wave Reflection in Opposing Variable Current

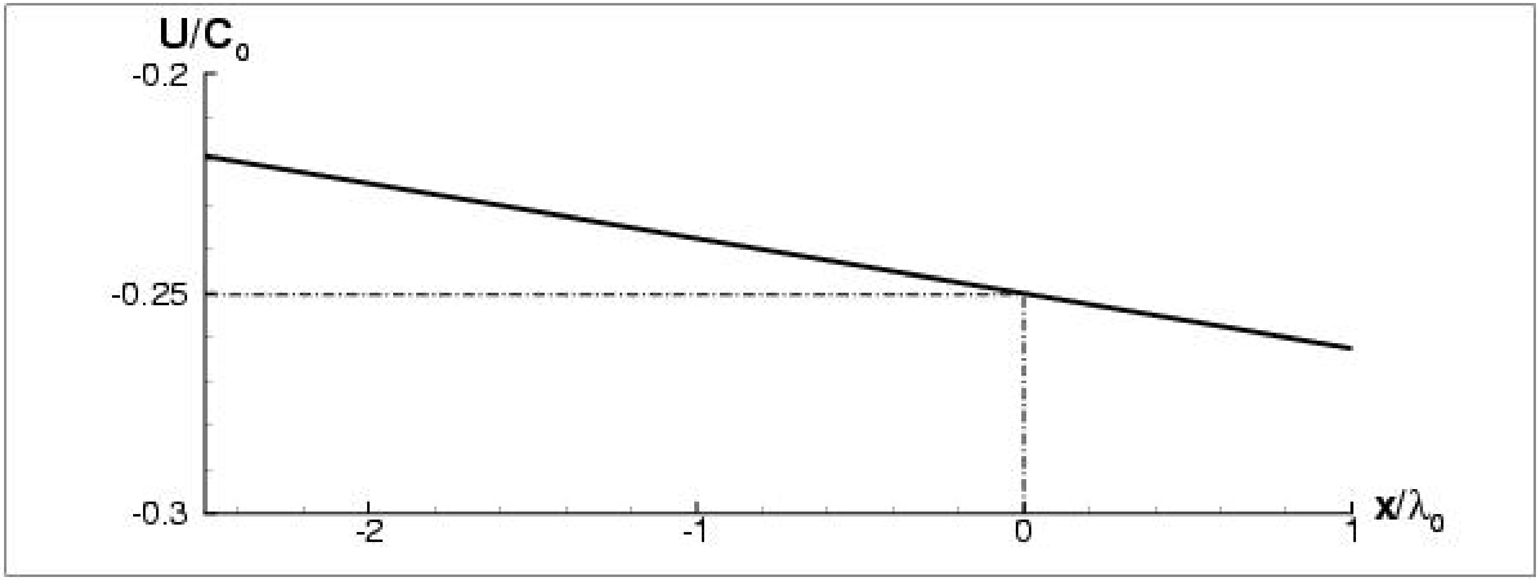

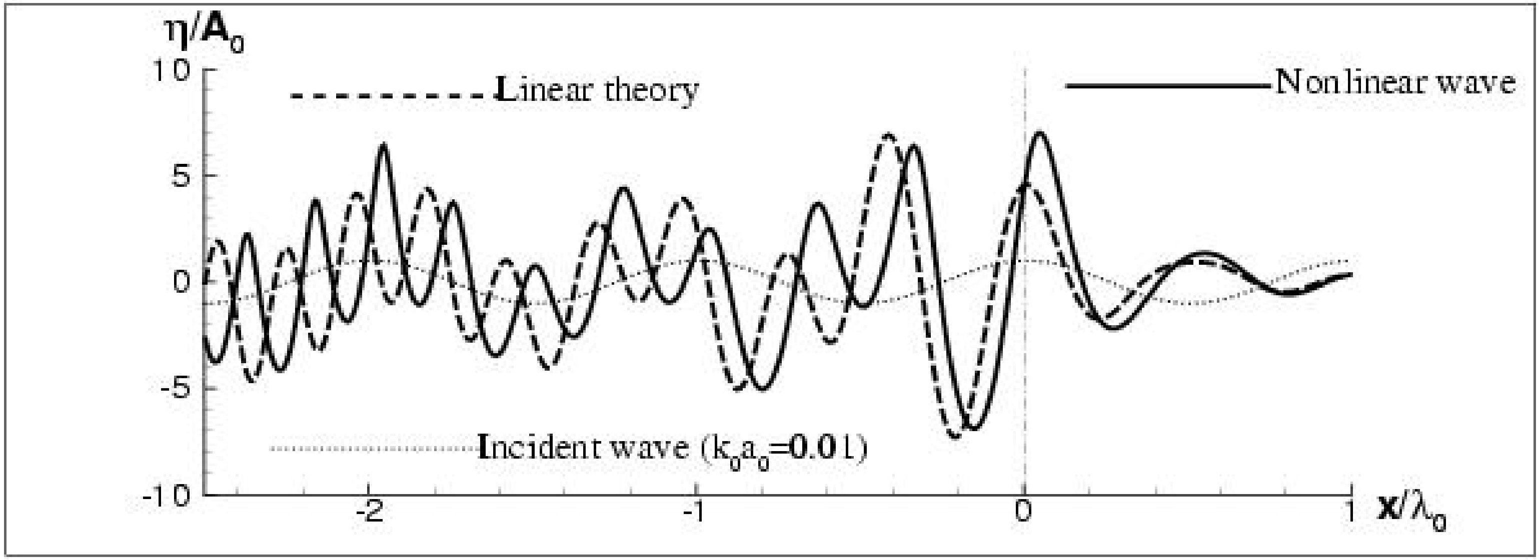

Nonlinear Wave-Current Interaction

Nonlinear evolution of a 3D irregular wave-field passing over a variable current field:

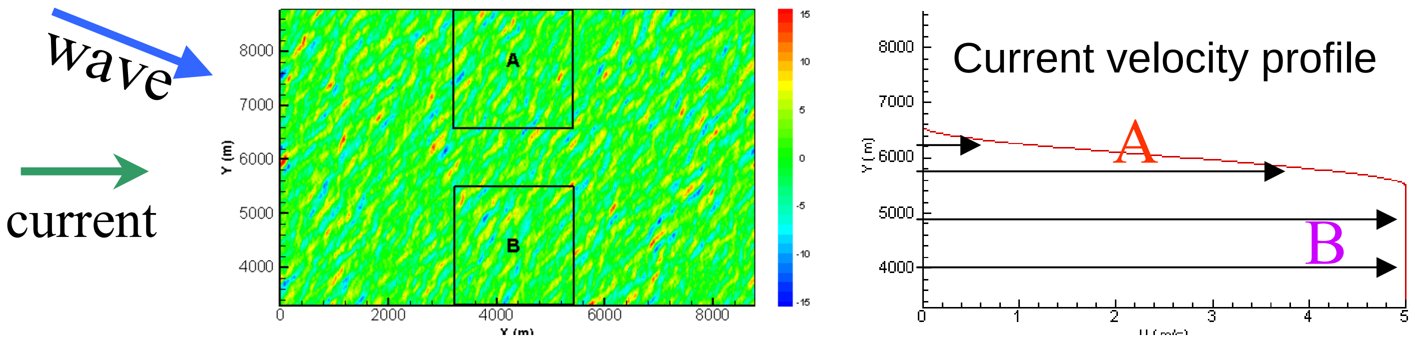

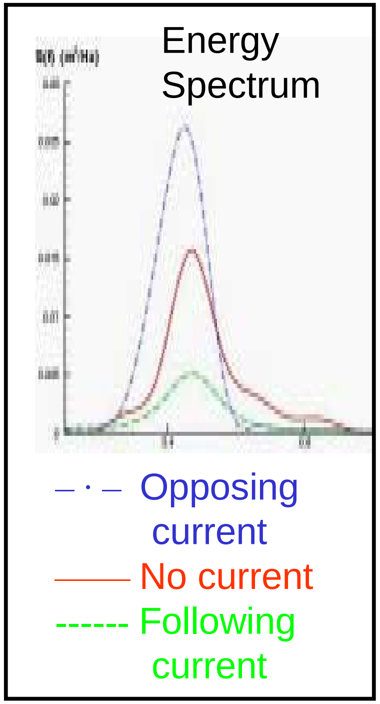

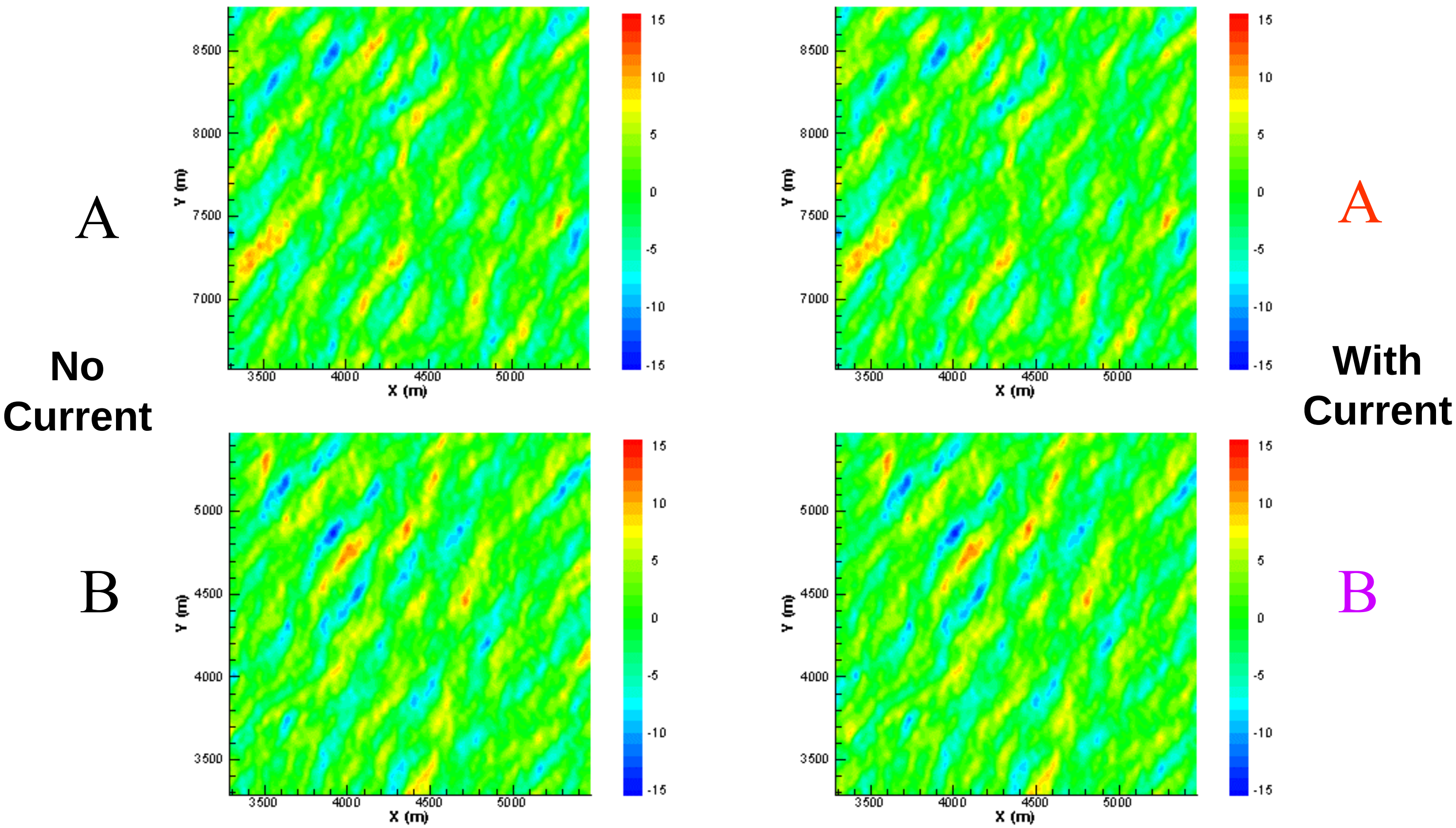

- ***Inclusion of current effect is important to wave prediction***

Deterministic Wave Reconstruction/Forecasting Using Composite Sensing Data

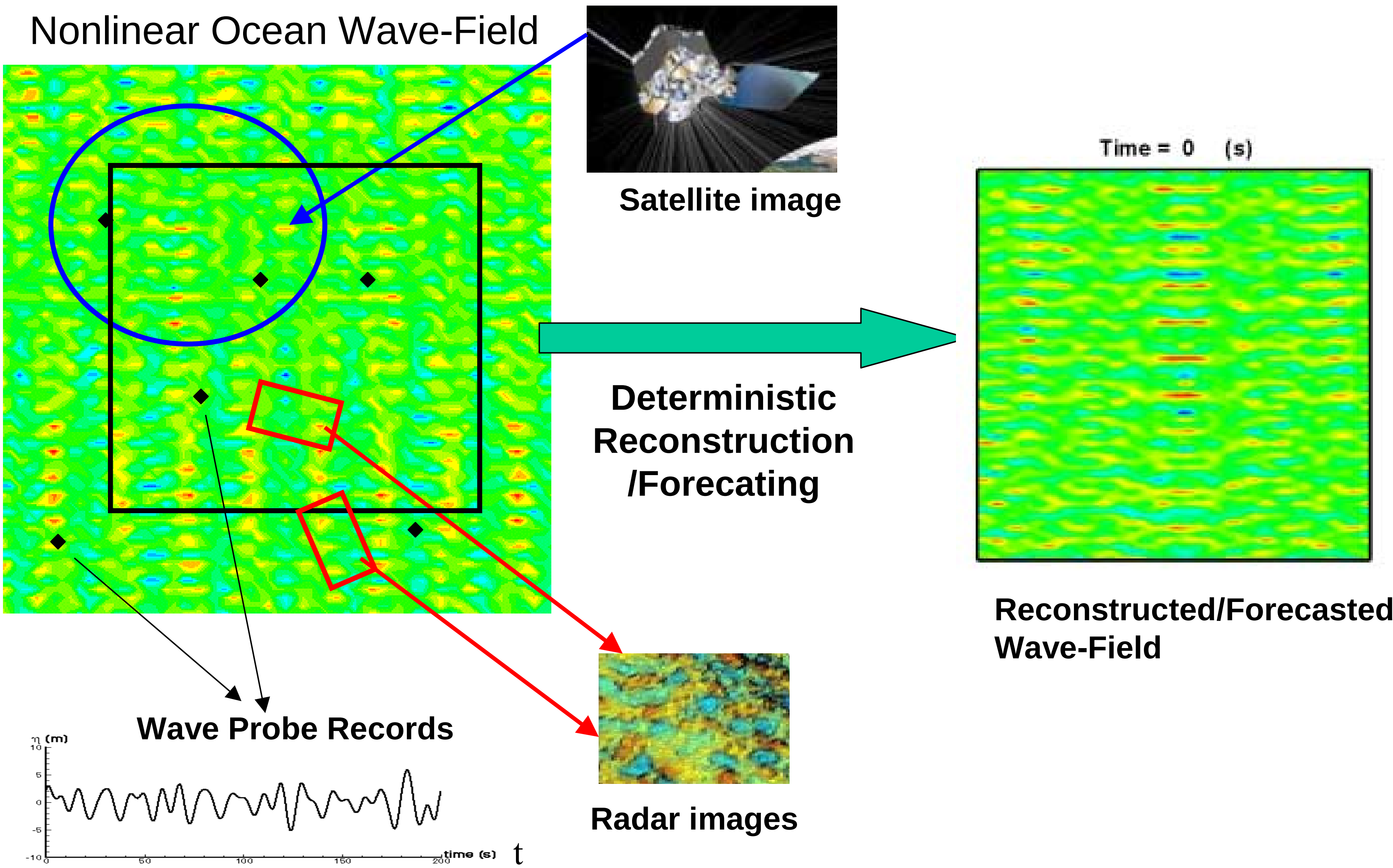

Assumptions

- Wave spectrum is frequency band and directional spreading limited ($\omega \in (\omega_{min}, \omega_{max})$; $\theta \in (-\pi/2, \pi/2)$).
- No assumption of stationarity (in time) or homogeneity (in space) of the wave statistics.
- Measurement data is exact (error analysis has been performed using direct simulation Monte Carlo and polynomial chaos).
- No wind forcing, bottom friction and viscosity (so far).

Deterministic Wave Reconstruction Using Direct Multi-level Nonlinear Wave Prediction Models

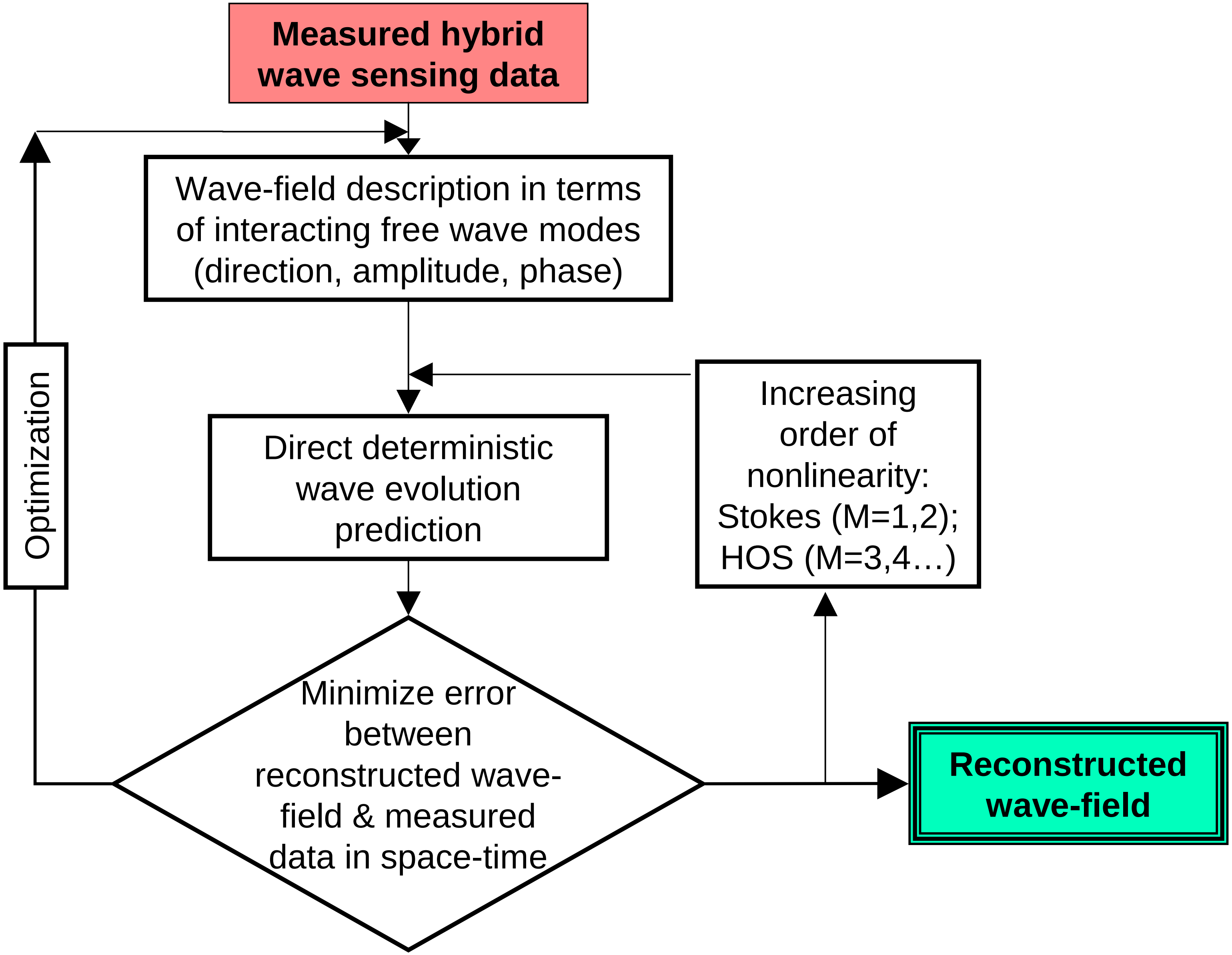

Comparison with Experiment

– Nonlinear Long-crest Wave Reconstruction

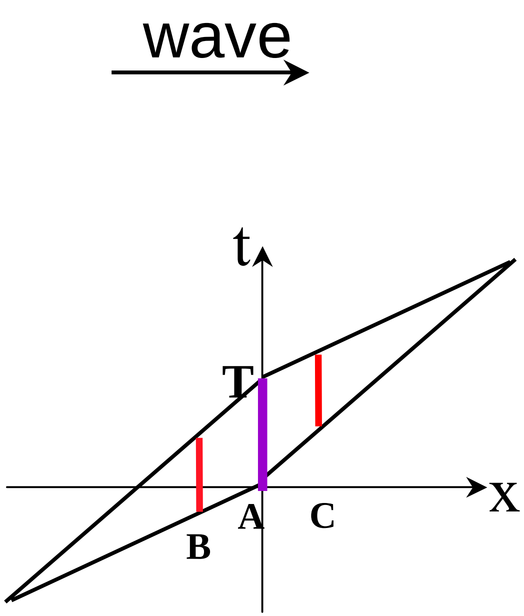

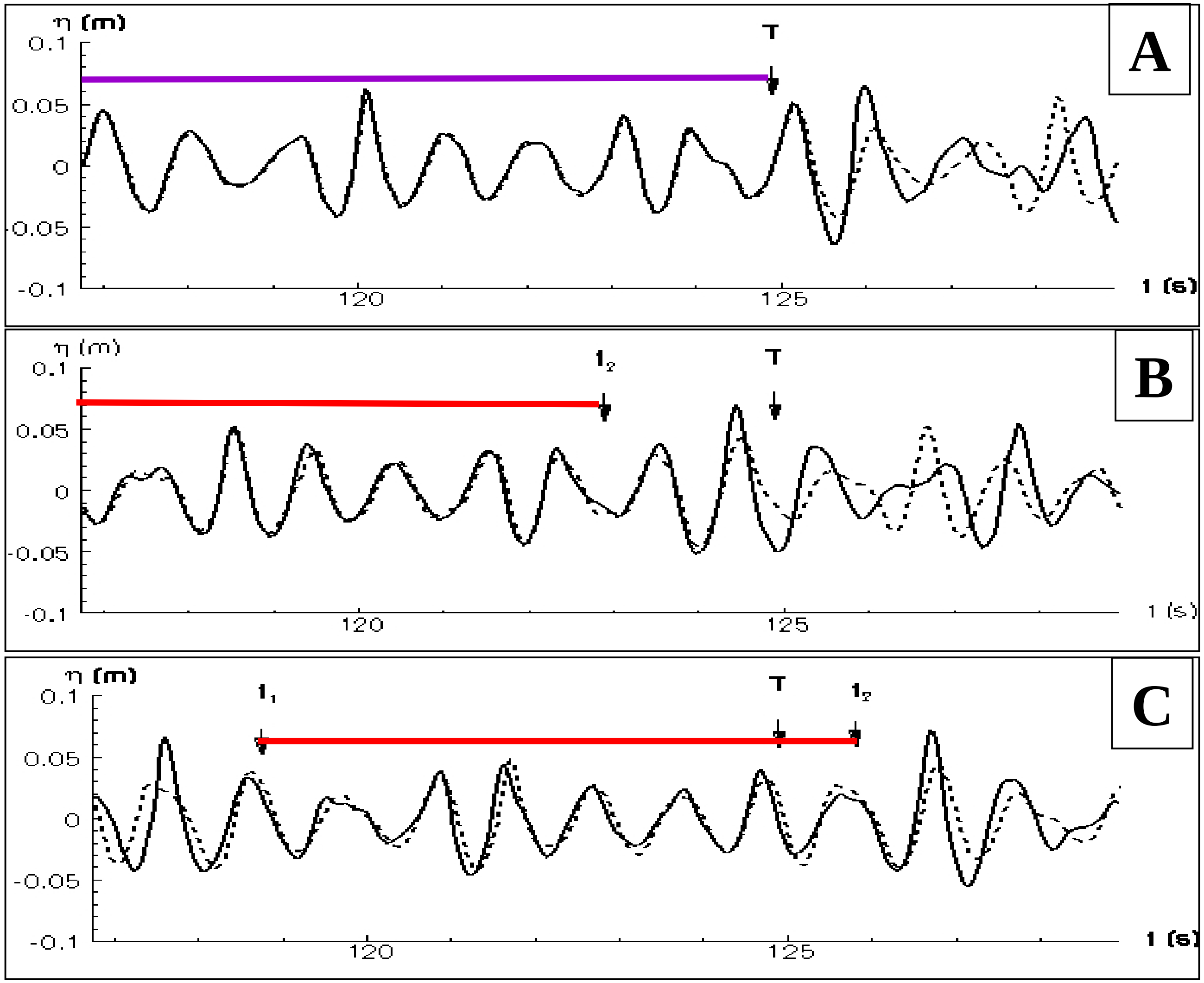

ka =0.23

Experiment (*TAMU, 2000*) — Reconstruction

Data used in reconstruction — Predictable region

Nonlinear Effect on Space-Time Predictable Region

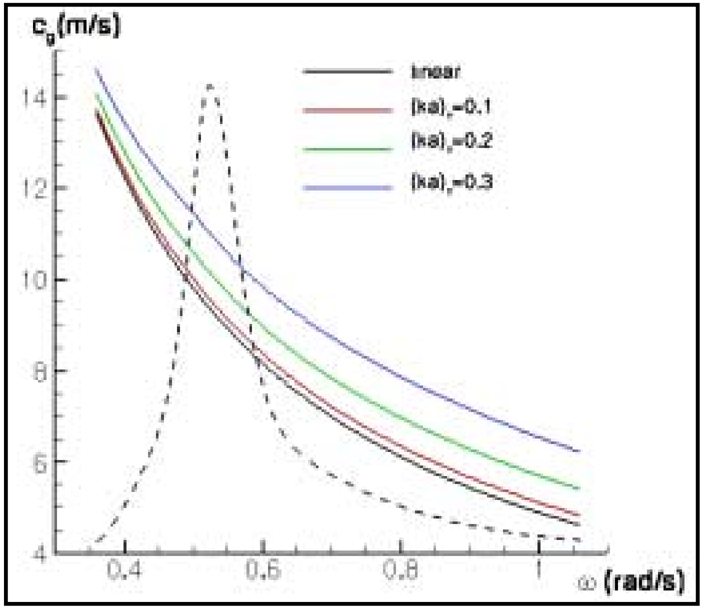

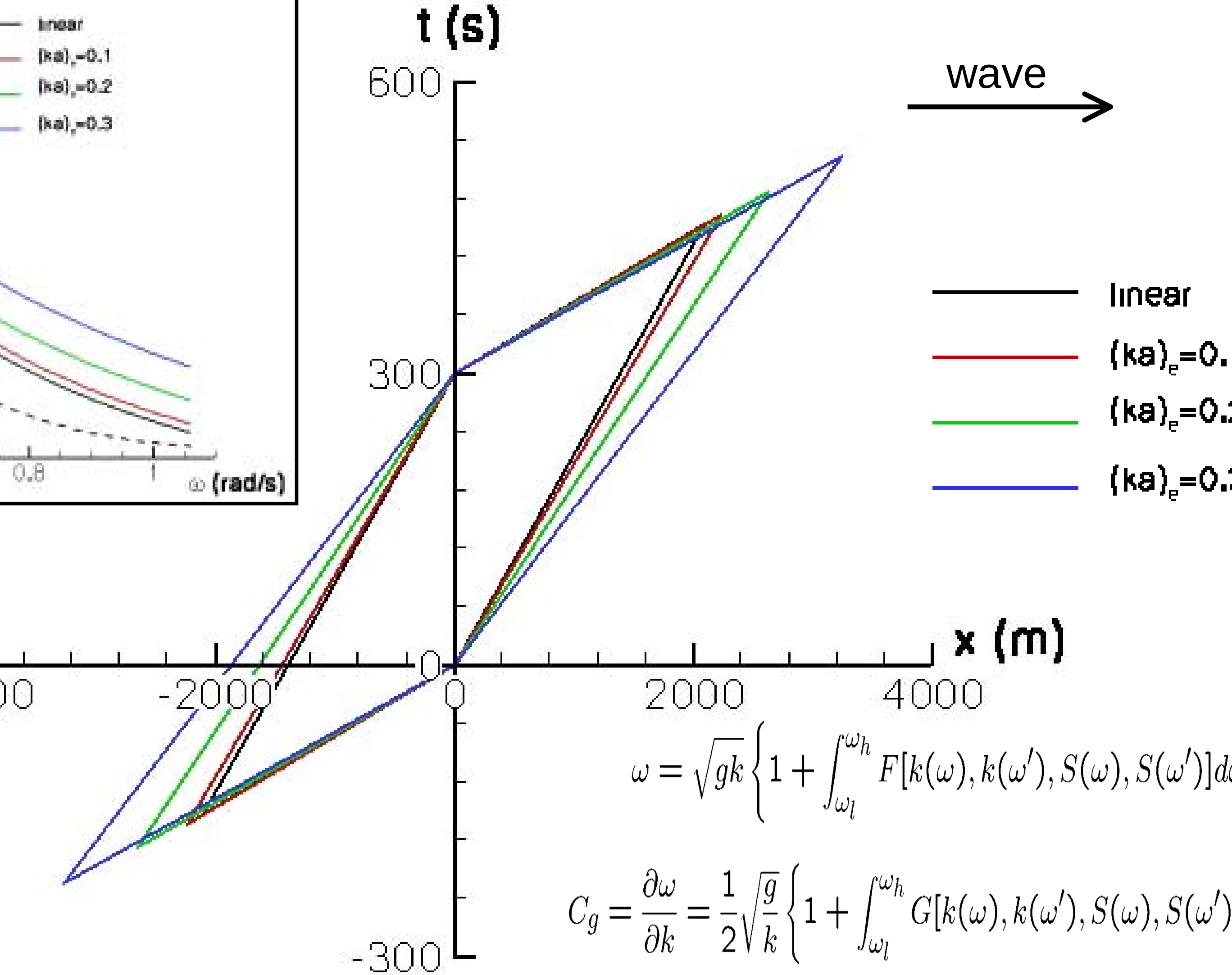

$$\omega = \sqrt{gk}\left\{1 + \int_{\omega_l}^{\omega_h} F[k(\omega), k(\omega'), S(\omega), S(\omega')]d\omega\right\}$$

$$C_g = \frac{\partial \omega}{\partial k} = \frac{1}{2}\sqrt{\frac{g}{k}}\left\{1 + \int_{\omega_l}^{\omega_h} G[k(\omega), k(\omega'), S(\omega), S(\omega')]d\omega\right\}$$

- **Nonlinearity increases the predictable region by making the group velocity of different wave components closer to each other**

Comparison with Experiment – Wave Kinematics

***ka* = 0.1**

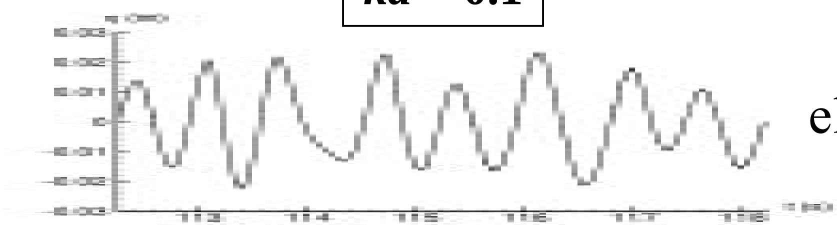

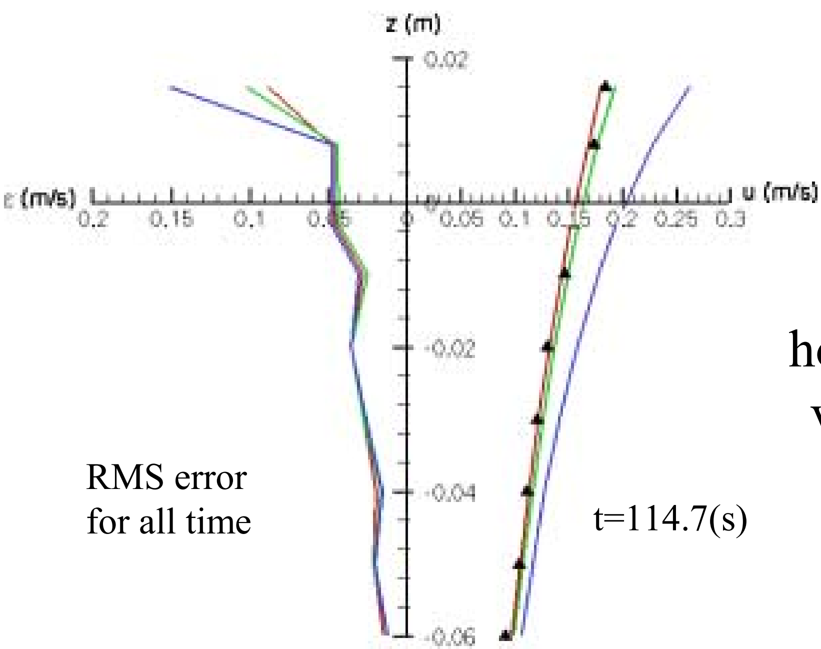

elevation

horizontal velocity

***ka* = 0.23**

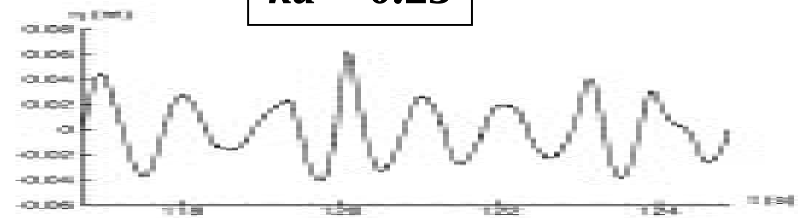

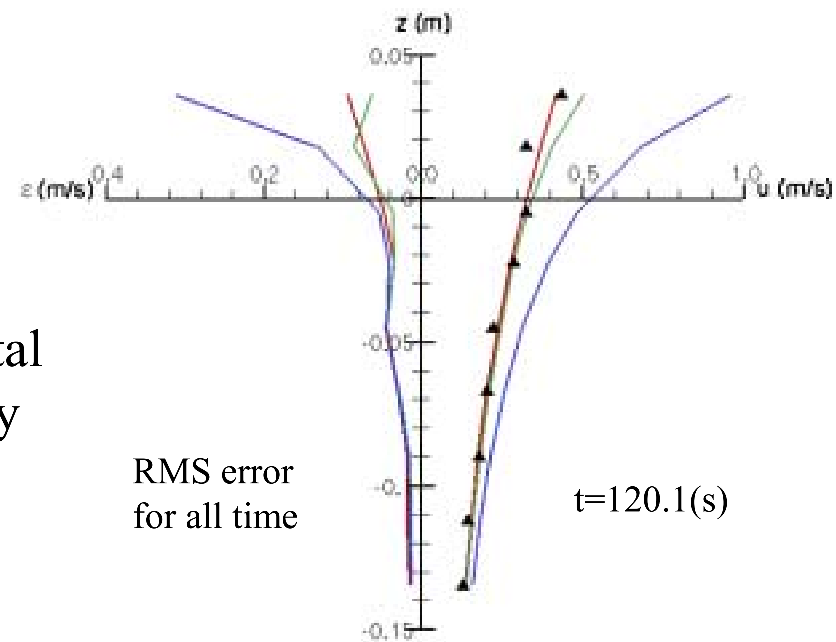

▲ ▲ ▲ Experiment (*TAMU, 2000*)

Linear

HOS

Second-order

Comparison with Experiment – Wave Forces

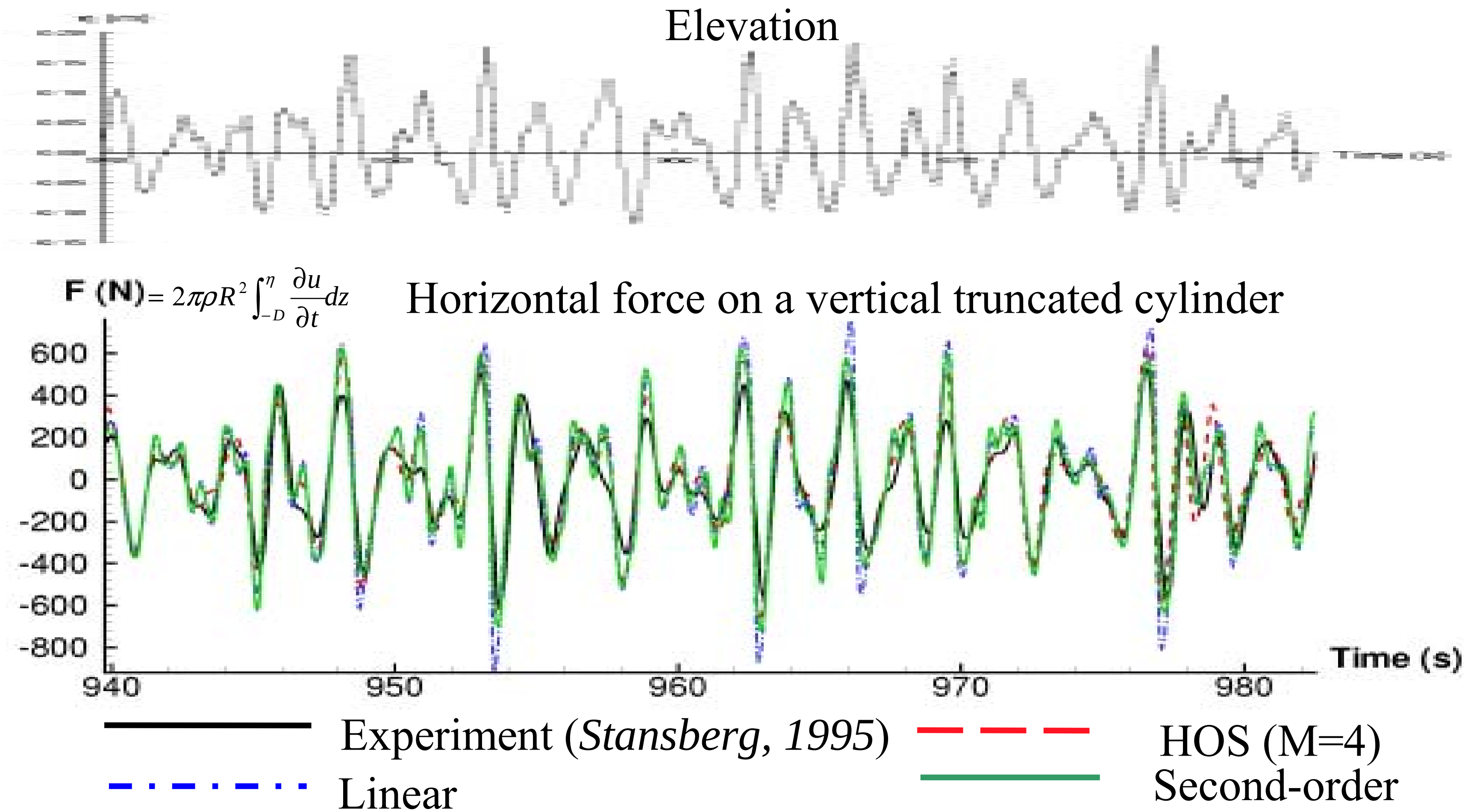

Wave nonlinearity is <u>critical</u> for *deterministic* reconstruction/forecasting:

- (even) for relatively moderate seas
- for large space-time evolution (nonlinear phase speeds & resonances)

Reconstruction and Forecasting of Long-Crested Irregular Waves

Used: 3 minutes (0-180 sec) of probe data at **A**

Forecast/Comparison: Wave elevation at downstream locations **B** (+500m) and **C** (+1 km)

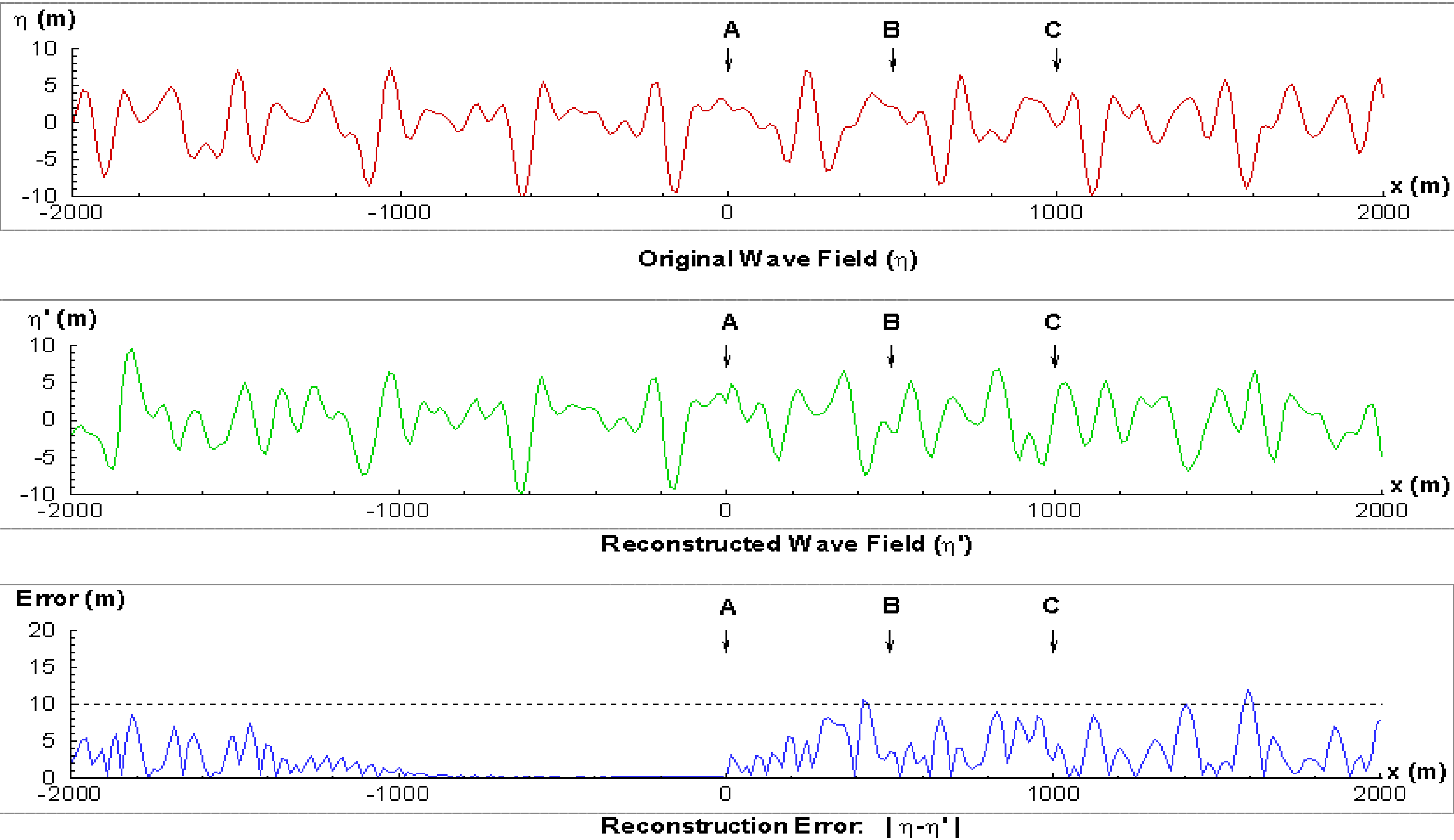

Extension to Short-crested Waves

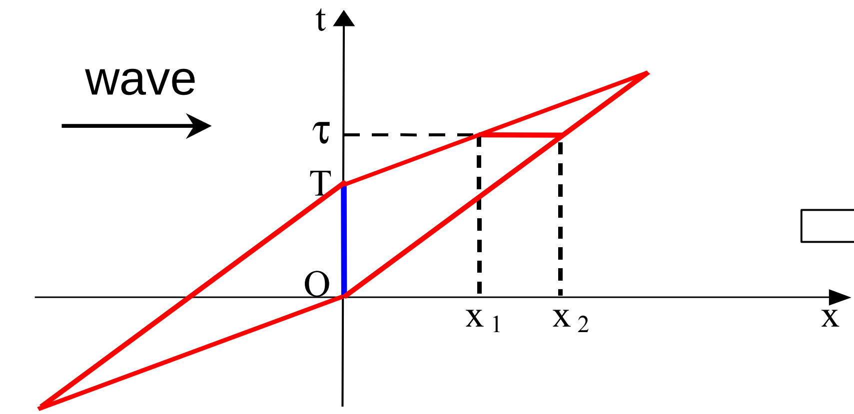

Unidirectional wave

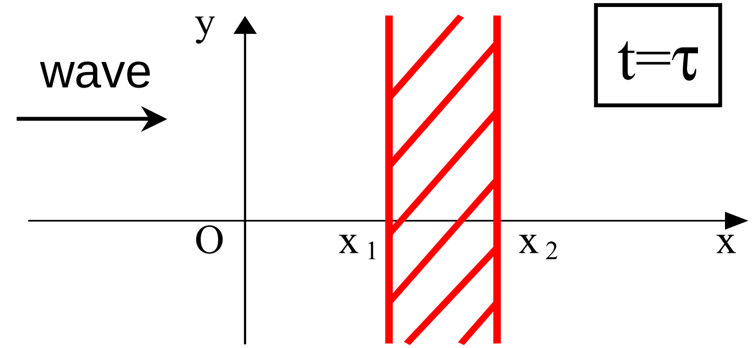

Unidirectional wave: in x-y space at time τ

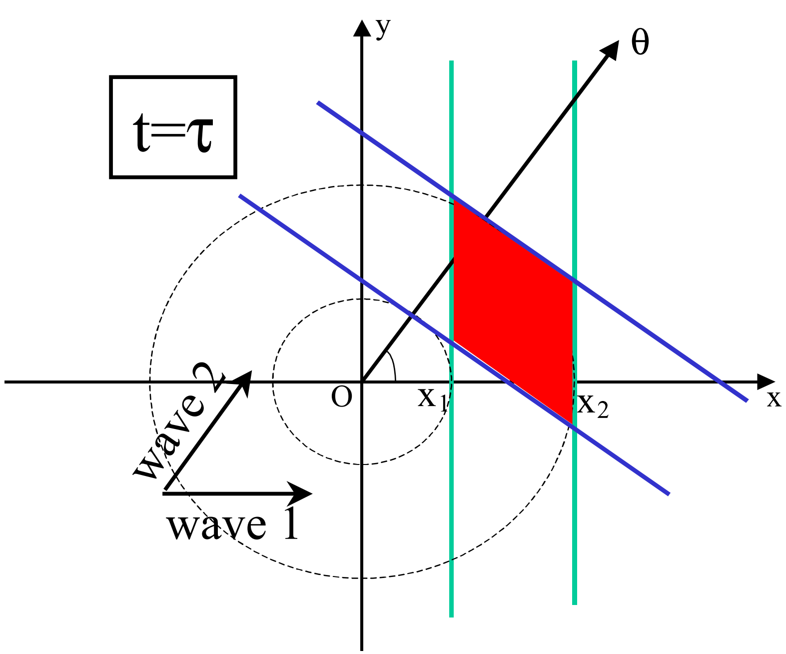

Waves propagating in two directions:
Positive-x direction and θ direction

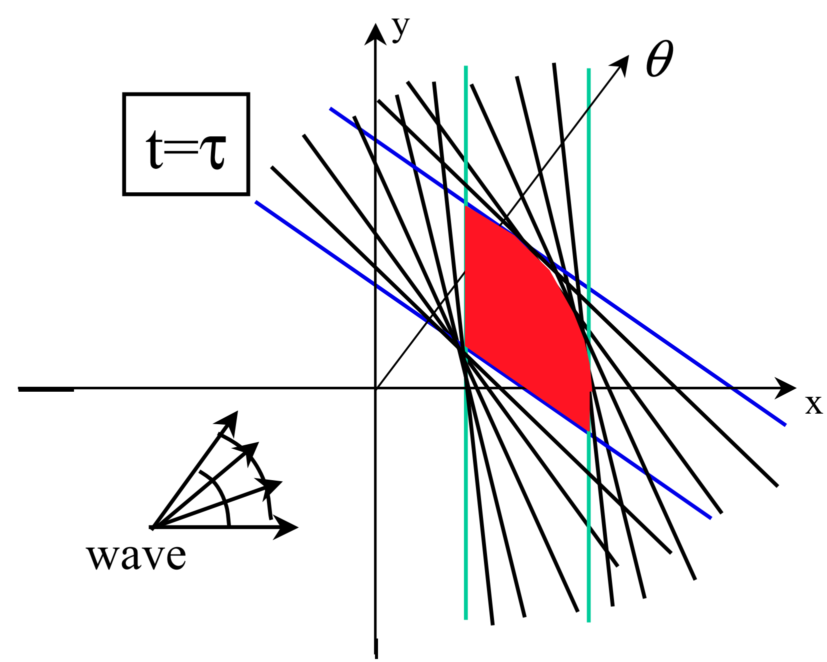

Wave propagating within
angle range [0, θ]

Space-Time Predictable Region for Short-Crested Waves

Elevation data given at a single point: $\eta(x=0,\ y=0,\ t\in[0,T_0])$

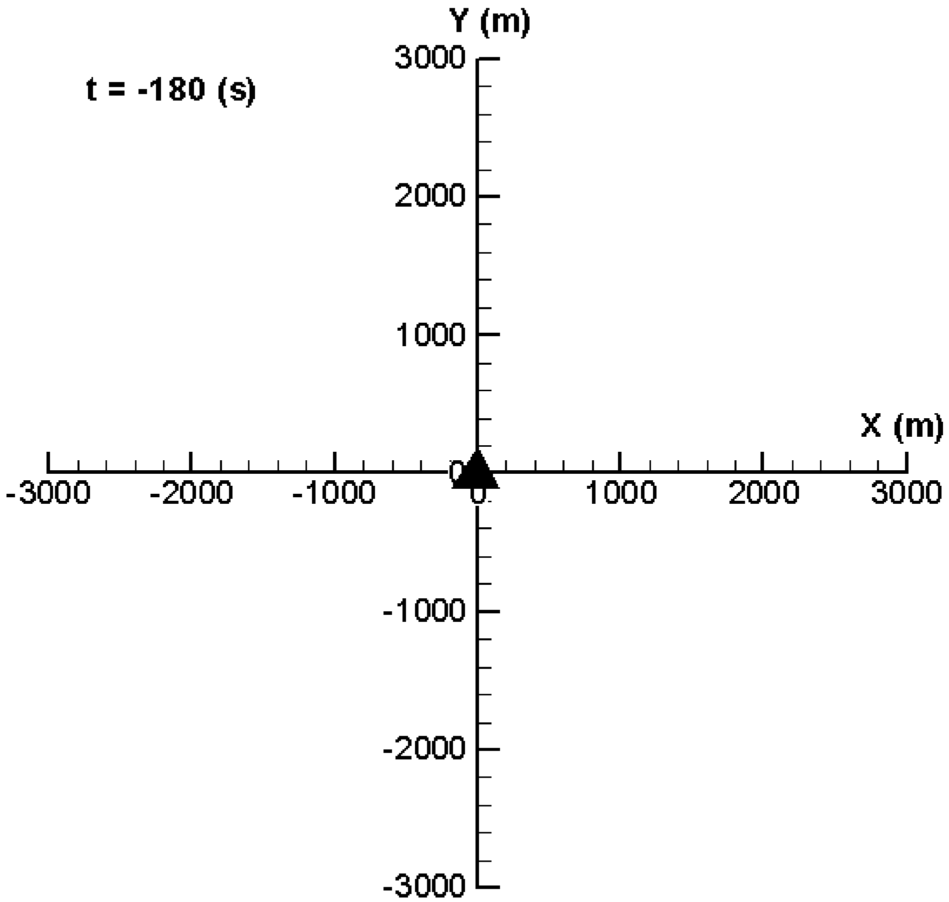

Reconstruction of a short-crested wave-field using multiple probes

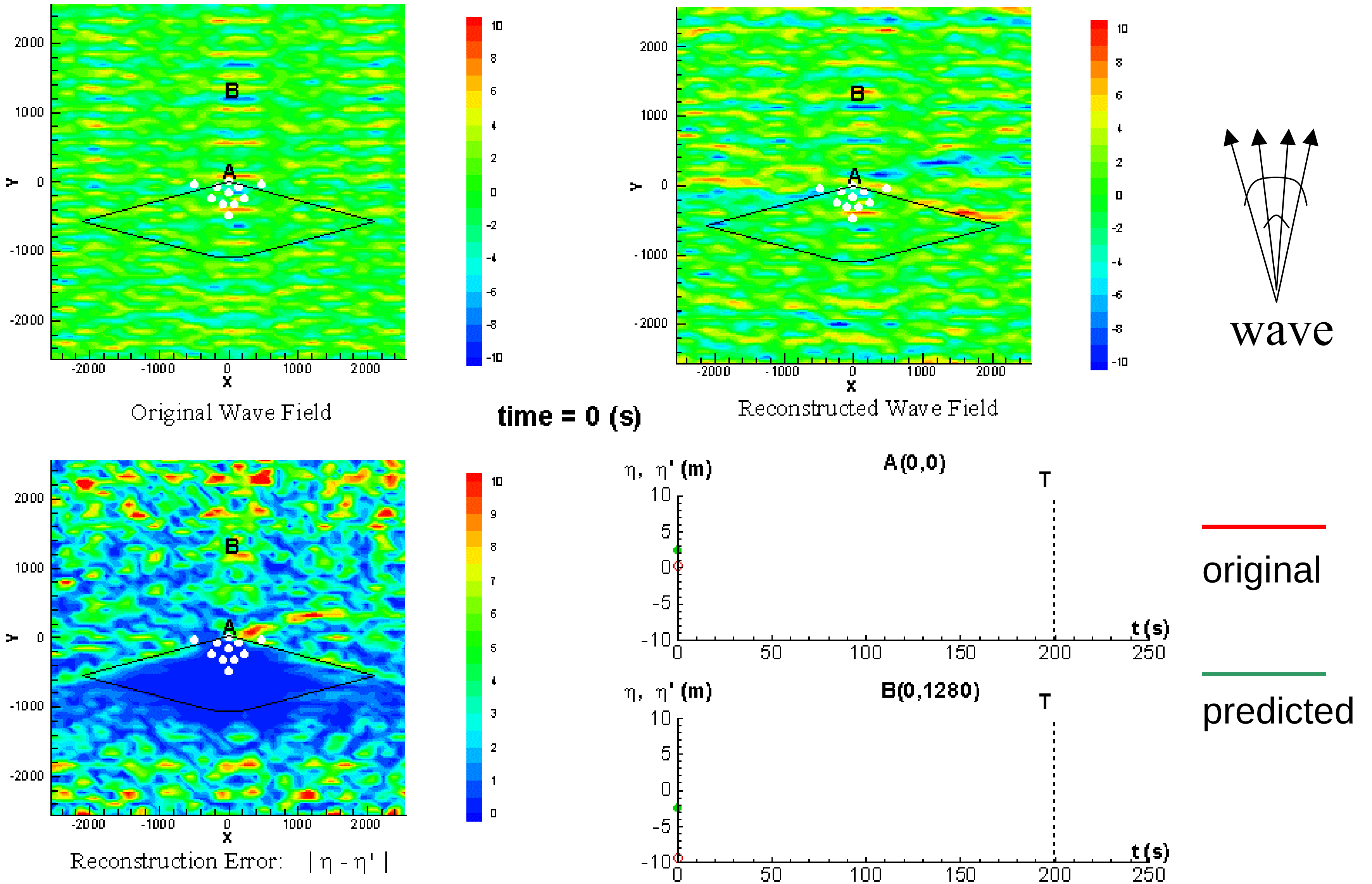

Comparison with Experiment
– Reconstruction of Nonlinear "Bull's Eye" Wave-field

Snapshot of Bull's Eye Wave in Wave Basin (*TAMU, 1999*)

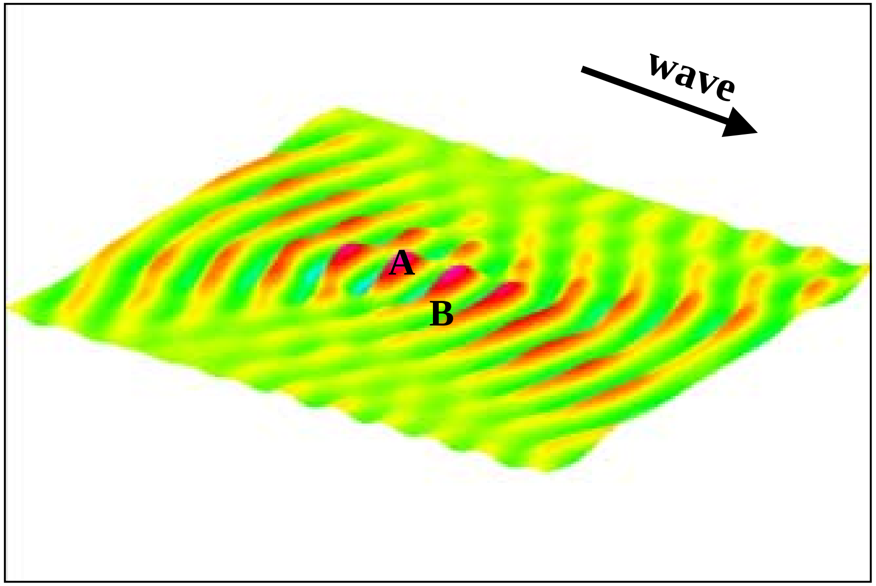

Reconstructed Nonlinear Wave-Field

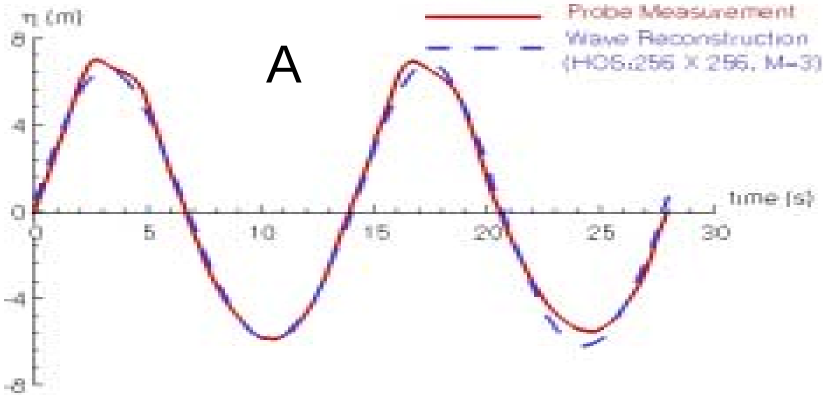

Sample Wave Record Used in Wave-Field Reconstruction

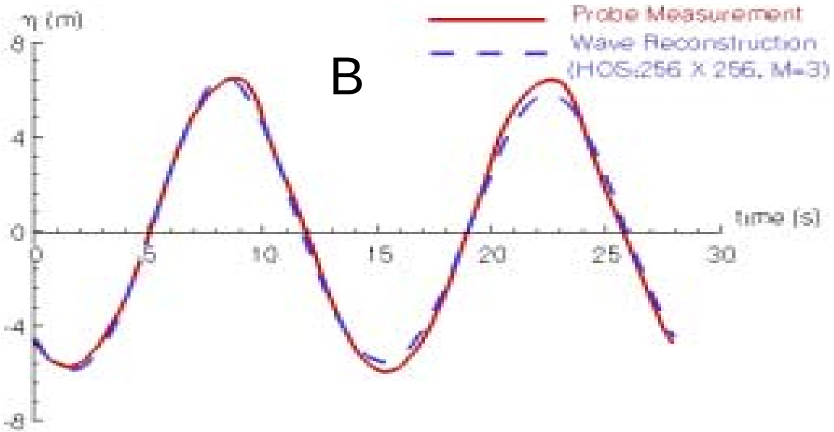

Comparison of HOS-Predicted and Measured Wave Time Record

Reconstruction and Forecasting of Short-Crested Irregular Waves

Using 13 *moving* probes: reconstruct a 10km $\times$ 3km wave-field around A
forecast wave-field in a region around B

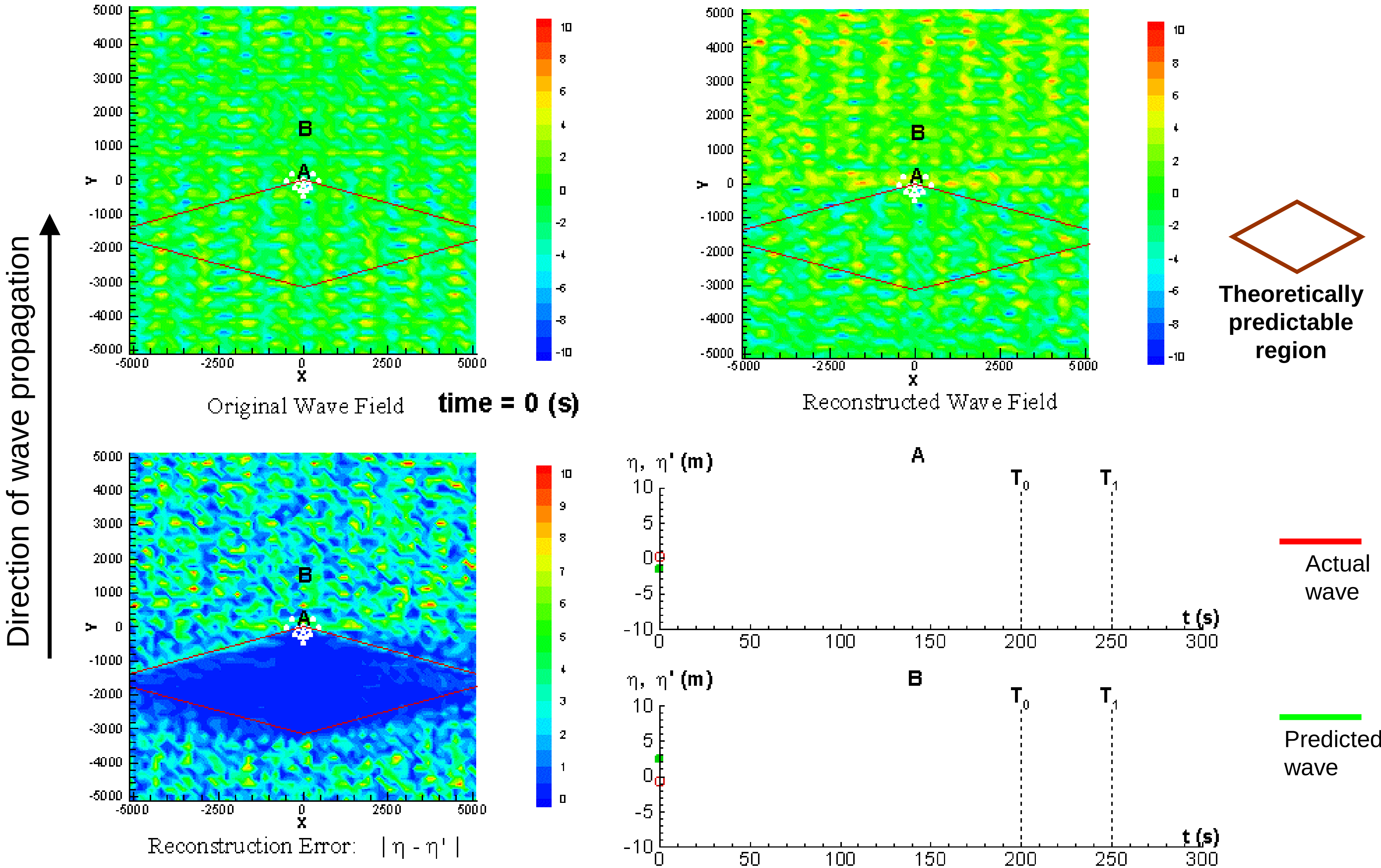

Simulation of Large-Scale Nonlinear Ocean Wave-Fields using High-Performance Computing (HPC)

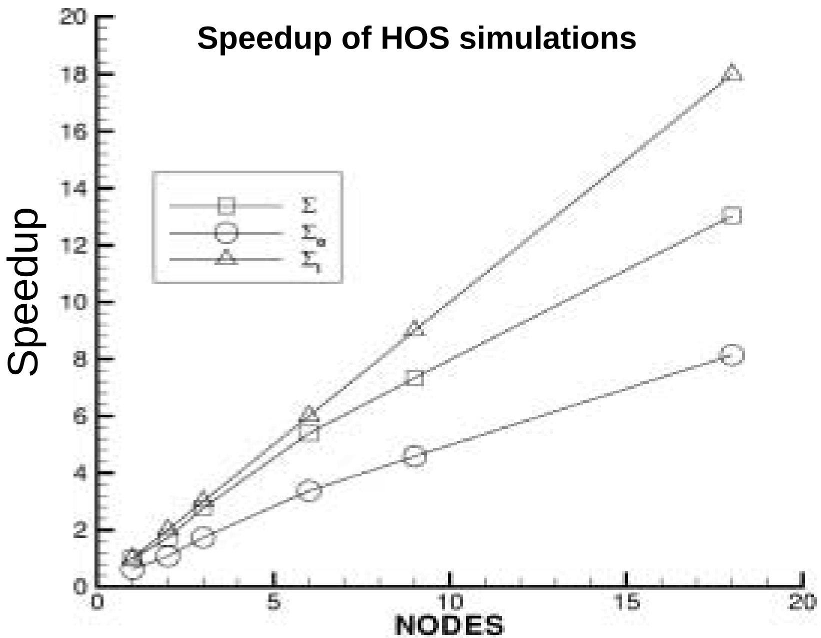

- **High scalability on modern high-performance parallel platforms (IBM SP3, Cray T3E)**
- **Up to 256 processors deployed to date; use of O(2000) processors in the immediate future**

Domain (km X km)	**Evolution Time (sec)**	**CPU(hr) "today"** Cray T3E, IBM SP3	**Simulation/Real Time** "today"	**12/04** (projected)	**9/05** (projected)
1 X 1	$O(10^2)$	~1	~0.2		
10 X 10	$O(10^3)$	$\sim10^3$	~20	~2	
30 X 30	$O(10^{3\sim4})$	$10^{4\sim5}$	~500	~20	~1
100 X 100	$O(10^{4\sim5})$	$10^{5\sim6}$	~5000	~200	~10

Direct Simulation of *Large-Scale* Nonlinear Ocean Waves

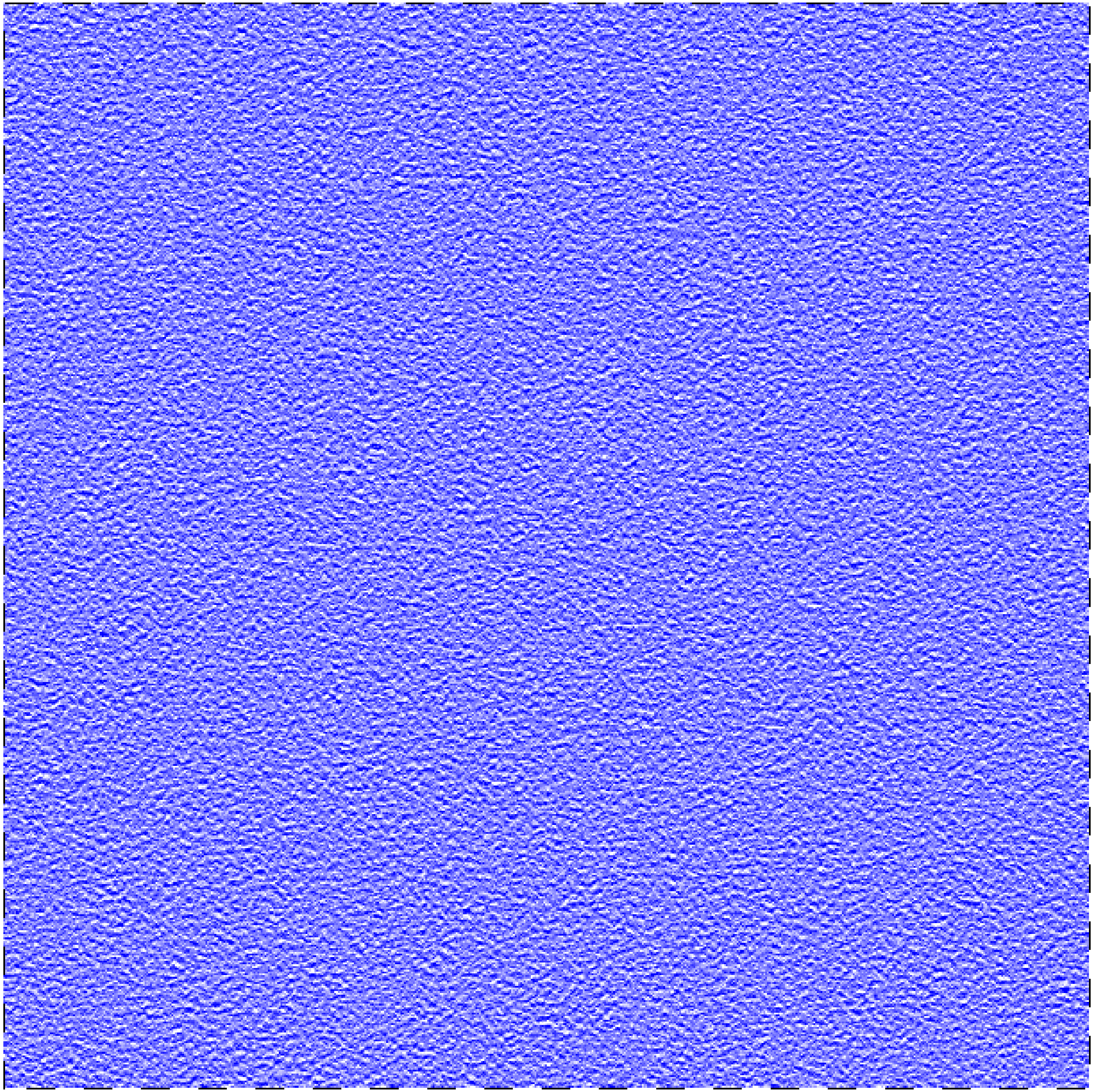

Domain: 30km $\times$ 30km
Evolution time: 0.5hour

Irregular short-crested wave-field, sea-state ~8 (T_p = 12s, H_s = 12m)

Wave modes, N = 1.6×10^7

Nonlinear order, M = 4

 # time steps ~ O(10^4)

Computing platform: Cray T3E with 256 processors

Simulation time: O(100) hours

Combining Nonlinear Wave Reconstruction/Forecasting with Large-Amplitude Ship Motions Simulations

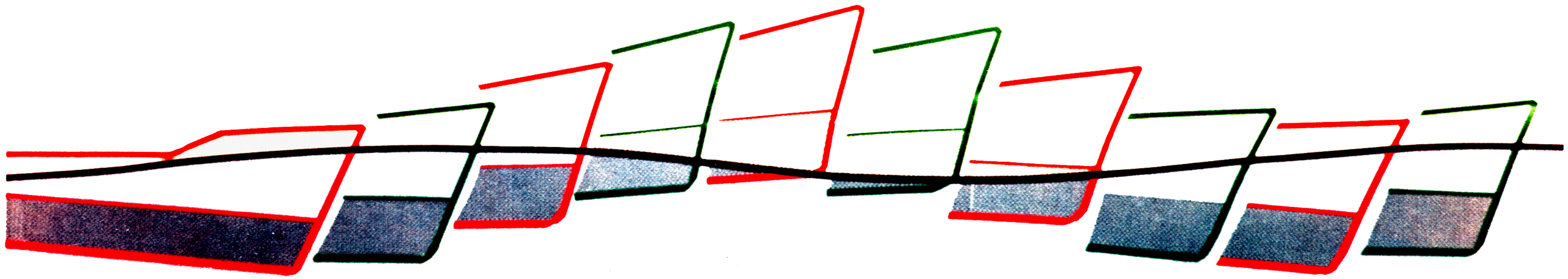

Using **L̲arge-A̲mplitude M̲otion P̲rogram (LAMP; Lin & Yue, 1990)** for vehicle dynamic simulation:

- A multi-level 3-D time-domain simulation system for nonlinear ship motions, wave loads, and structural responses.
- Using HOS wave-field kinematics for LAMP boundary condition on the ship hull.

Examples of LAMP Vehicle Dynamics Simulations

Parametric Rolling & Green Water

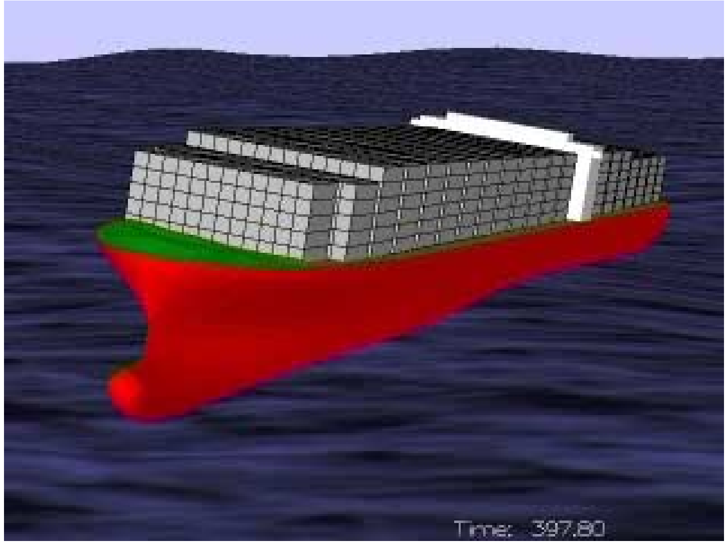

Planing Boat in Waves

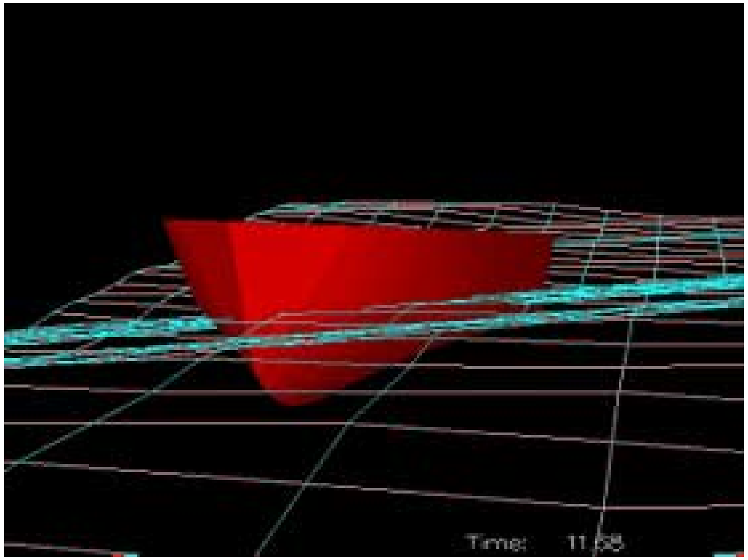

High Speed Multi-hulls

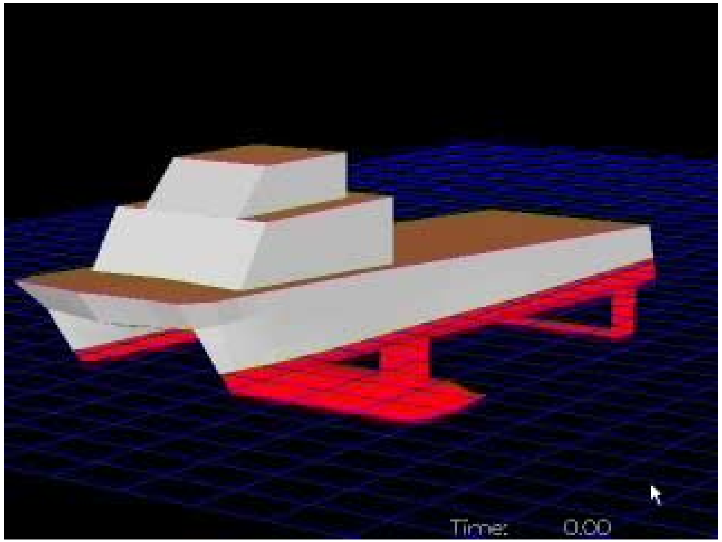

Ship-Ship Interaction

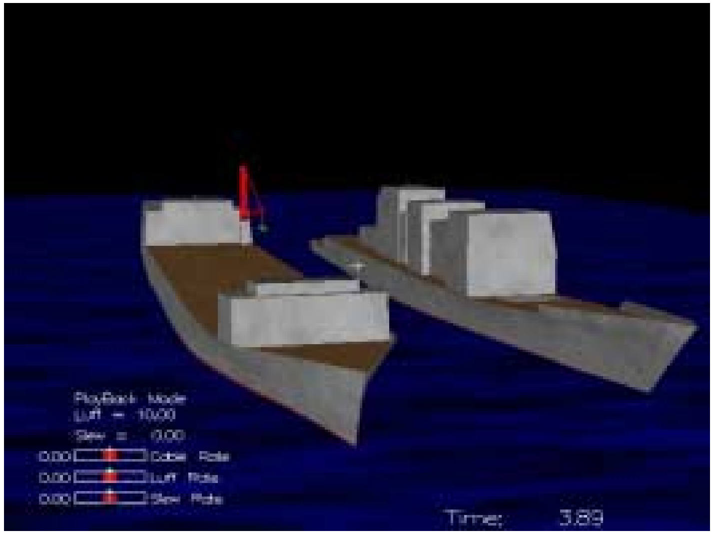

Incorporating Path Optimization and Rudder/Throttle Control to Enable SWASH

- Objective: To find optimal trajectories of vessels in waves, by combining *physical models* of high fidelity (LAMP) with accurate *environmental models (*wave reconstruction and wind)
- Available Methods for Optimization:
  - **Maximum Principle** (Pontryagin) - continuous or discrete
  - **Dynamic Programming** (Bellman) - inherently discrete
- *Adaptive step-size time integration* is needed in highly dynamic and nonlinear ship motion prediction.
- Current Approach: Employ a standard gradient technique with variable gain, to optimize via the Maximum Principle. *Computation load is acceptable.*

Optimal Path Planning in Dynamically Evolving Environment

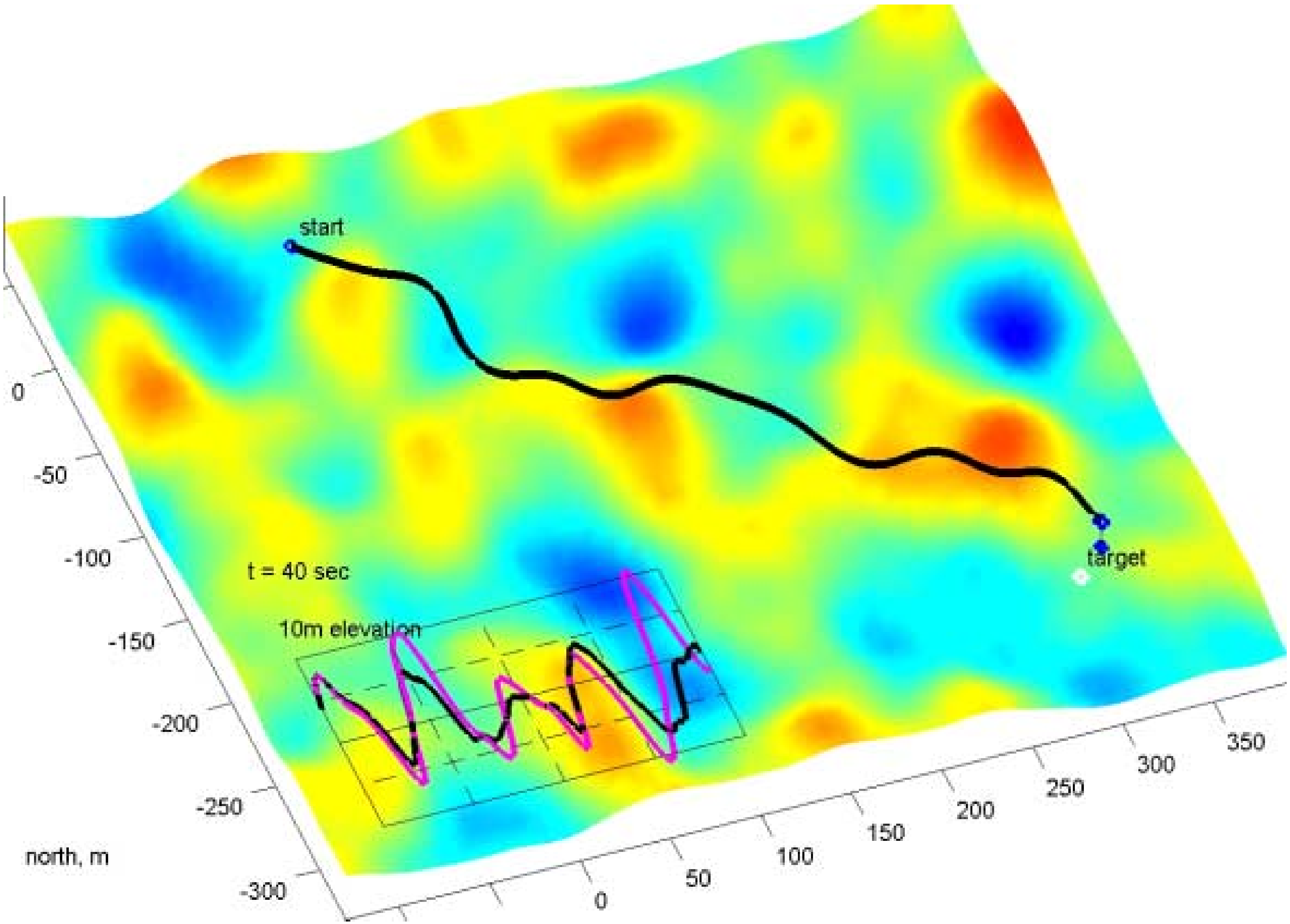

System Concept/Architecture

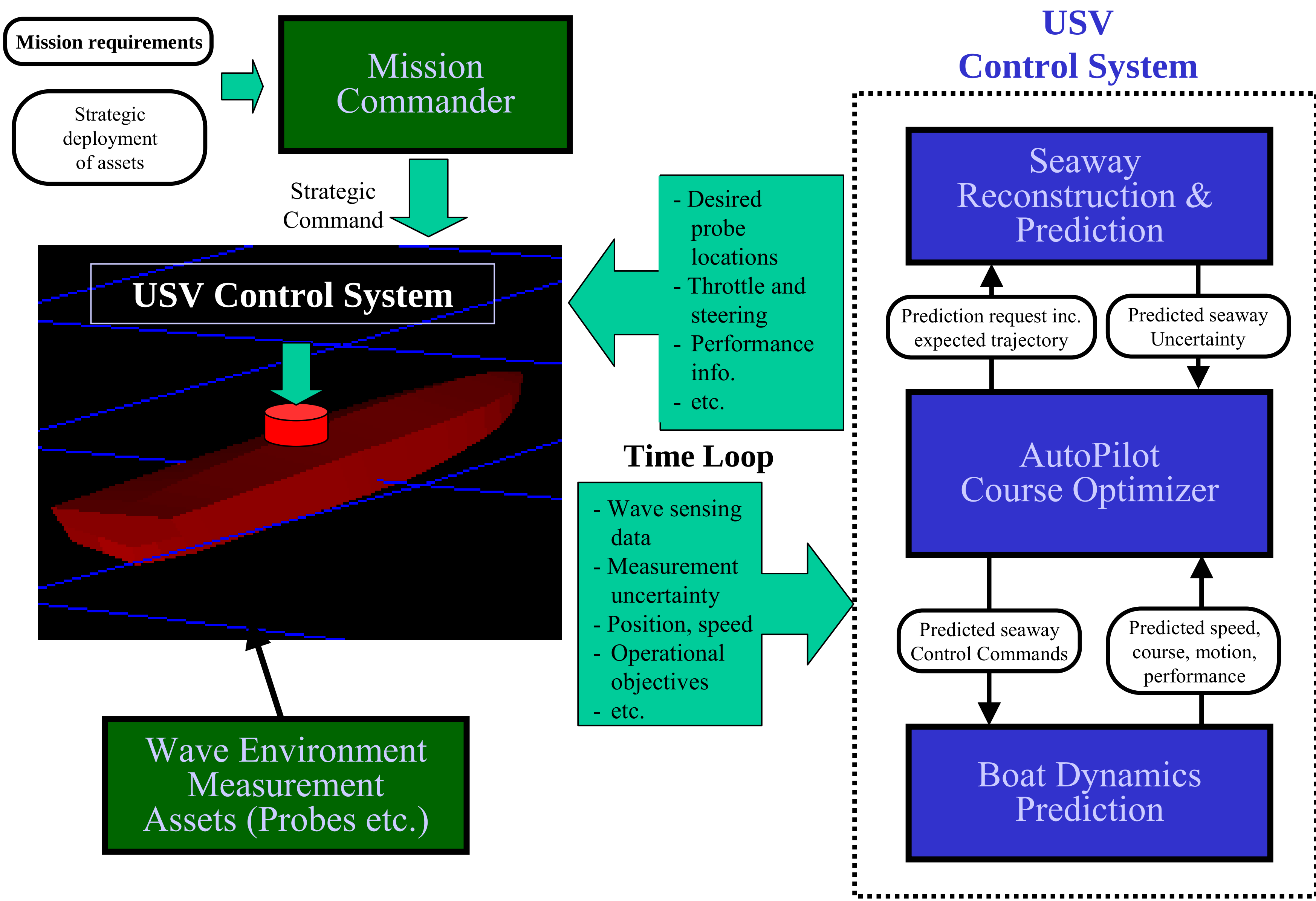

SWASH Demonstrations

Demo 1 – Small Vessel Operations in Waves

- 1.1 – Minimize overall rms motion in a transit (case I)
- 1.2 – Minimize overall rms motion in a transit (case II)
- 1.3 – Minimize motions in a specified time window

Demo 2 – Large Vessel Operation in Waves:
Assisted/automated helicopter landing and take-off

Demo 1.1: Minimize overall rms motion in a transit (case I)

Objective: Reduction of RMS Heave Motion in Point-to-Point Transit

Vessel: 7.2m RHIB, approx. 20 knots in SS4

Bearing: 45 degrees from head sea, average

Performance: Reduction of RMS heave from 0.51 to 0.34m: **34%**

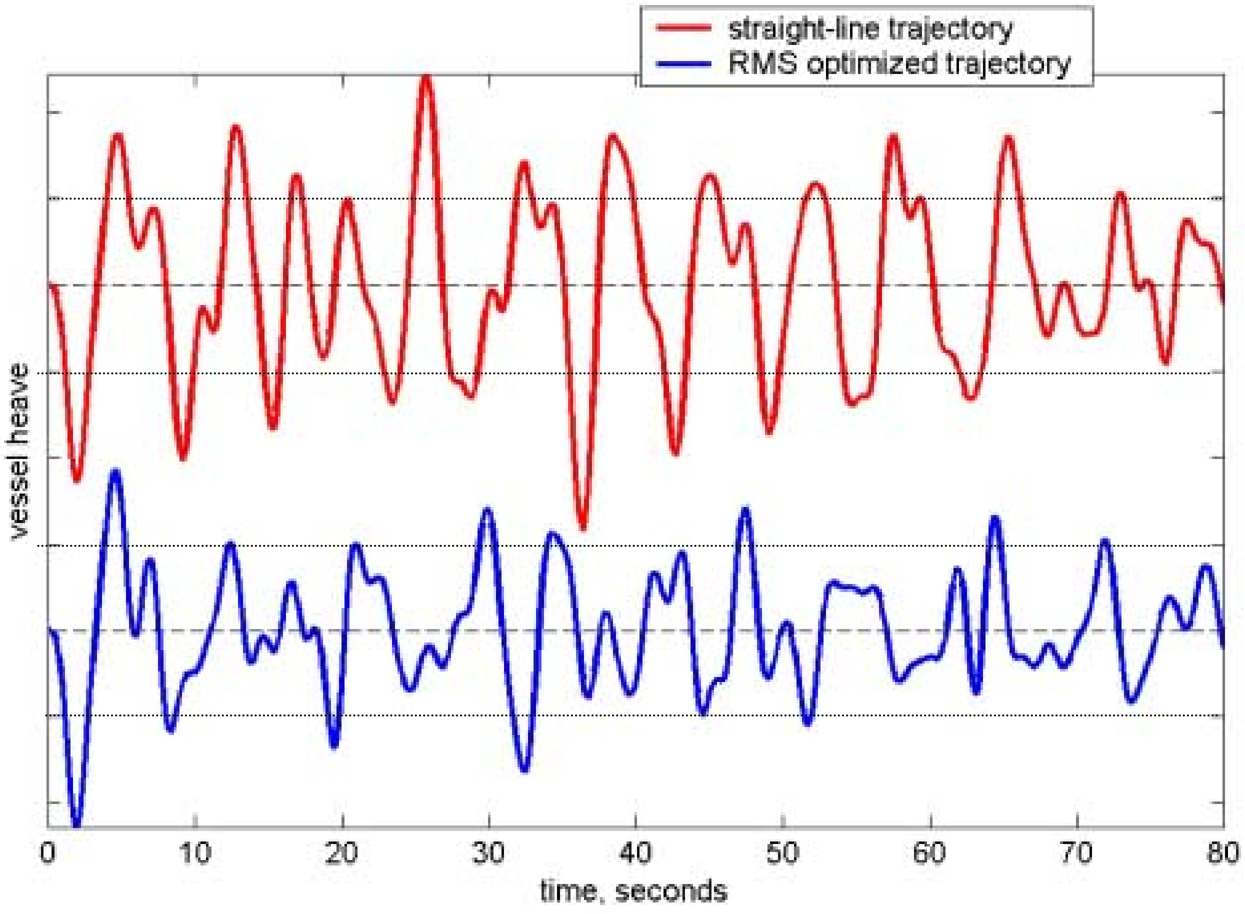

Demo 1.1: Minimize overall rms motion in a transit (case I)

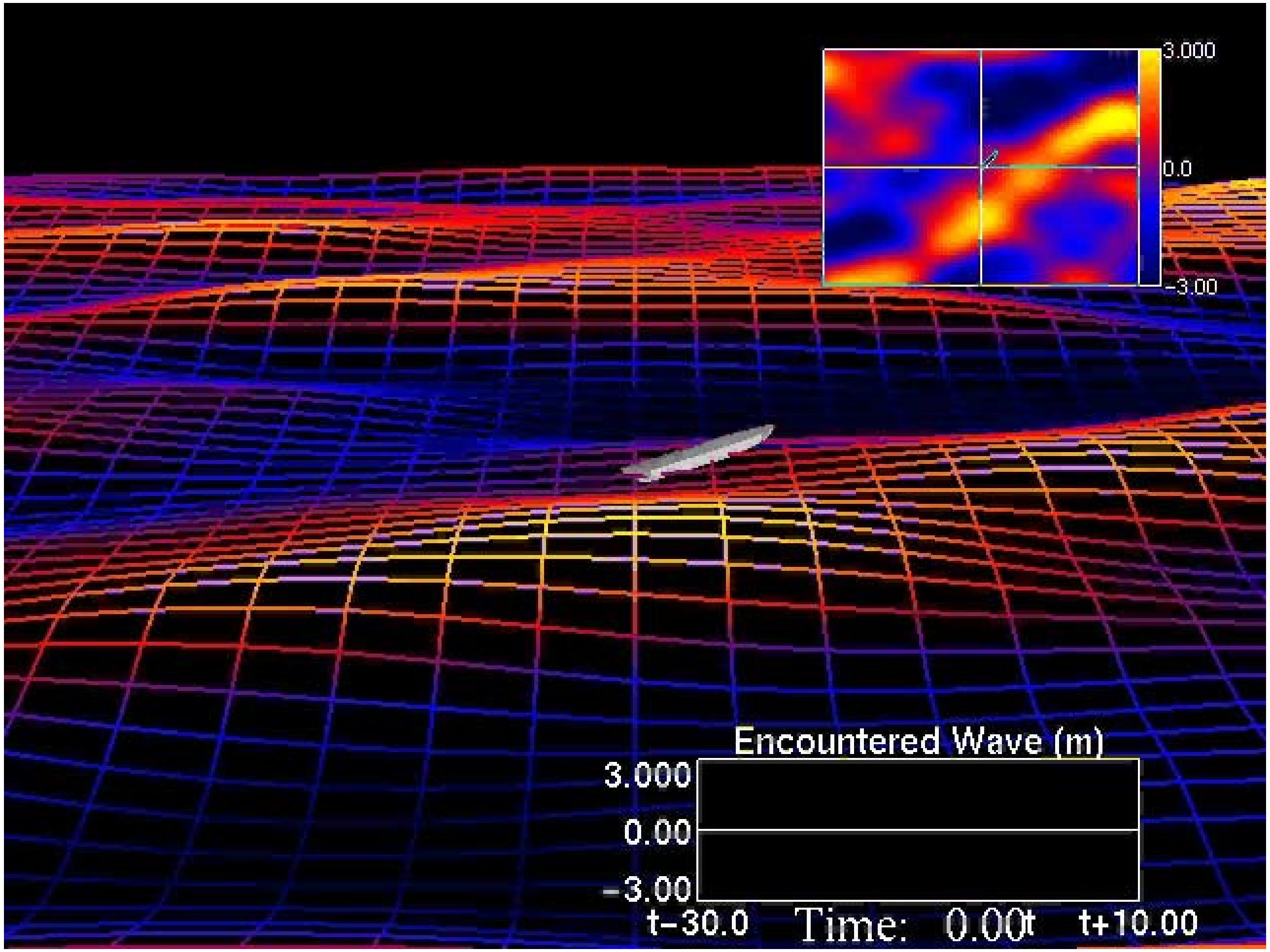

Demo 1.2: Minimize overall rms motion in a transit (case II)

Objective: Minimize rms vertical motions while trying to reach a given (possibly changing) destination within a fixed time.

Short-crested (60 deg spread) irregular seaway (wave heights up to 8 m)

Performance Comparison

RMS of wave…	Straight Course	With Path Opt	% reduction
Elevation	0.971 m	0.623 m	**36%**
Slope in axial dir	2.111 deg	1.116 deg	**48%**

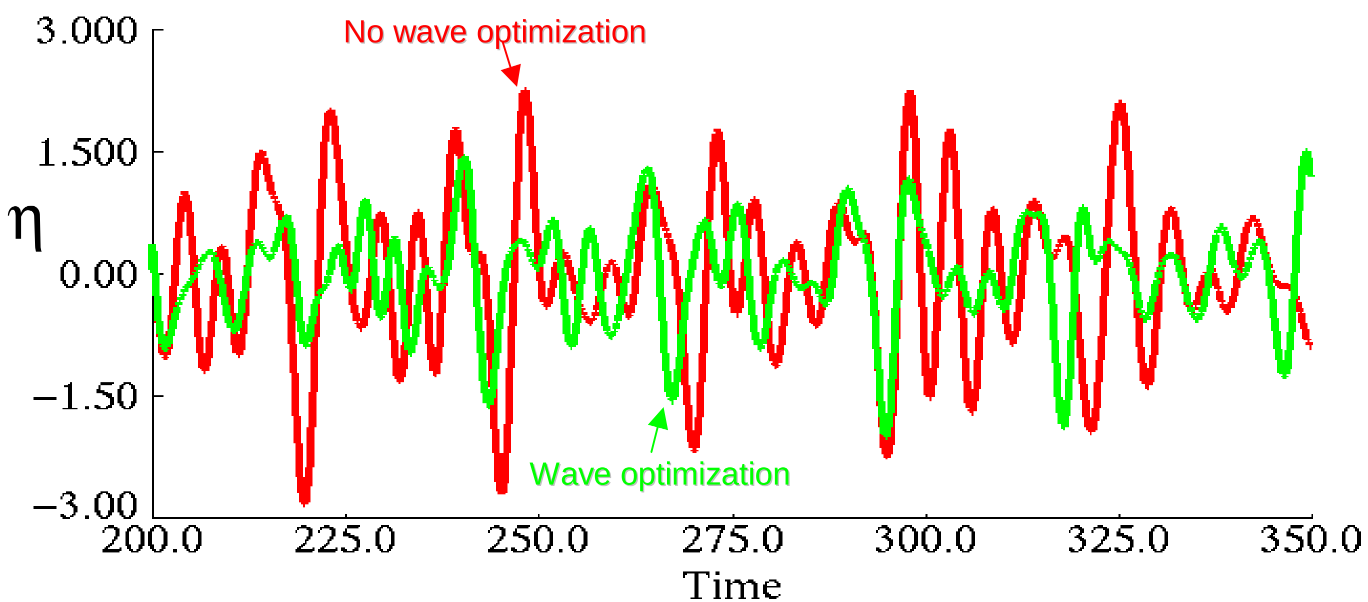

Demo 1.3: Minimize motions in a specified time window

Objective: Reduction of Peak Heave Acceleration in a Specific Time Window during Point-to-Point Transit

Vessel: 7.2m RHIB, approx. 20 knots in SS4

Bearing: 45 degrees from head sea, average

Performance: Reduction in window from 0.25g to 0.05g: **80%**

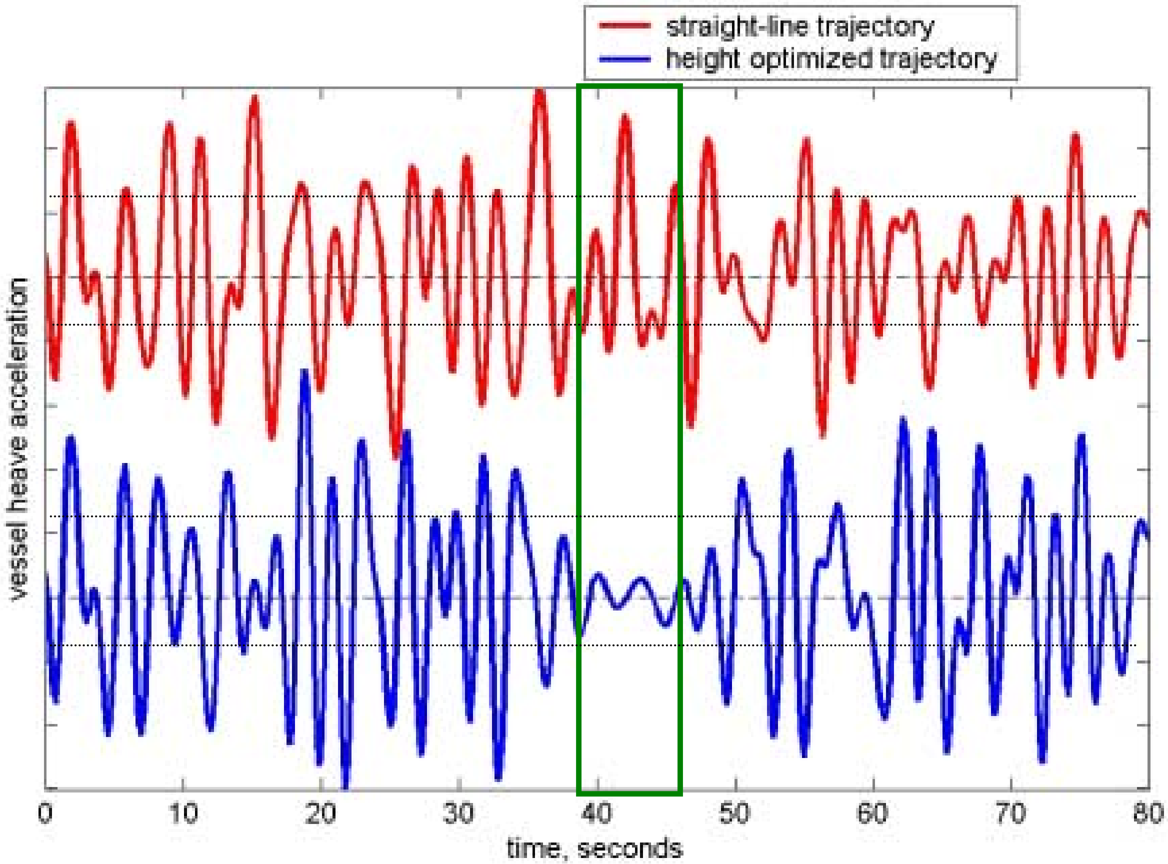

Demo 1.3: Minimize motions in a specified time window

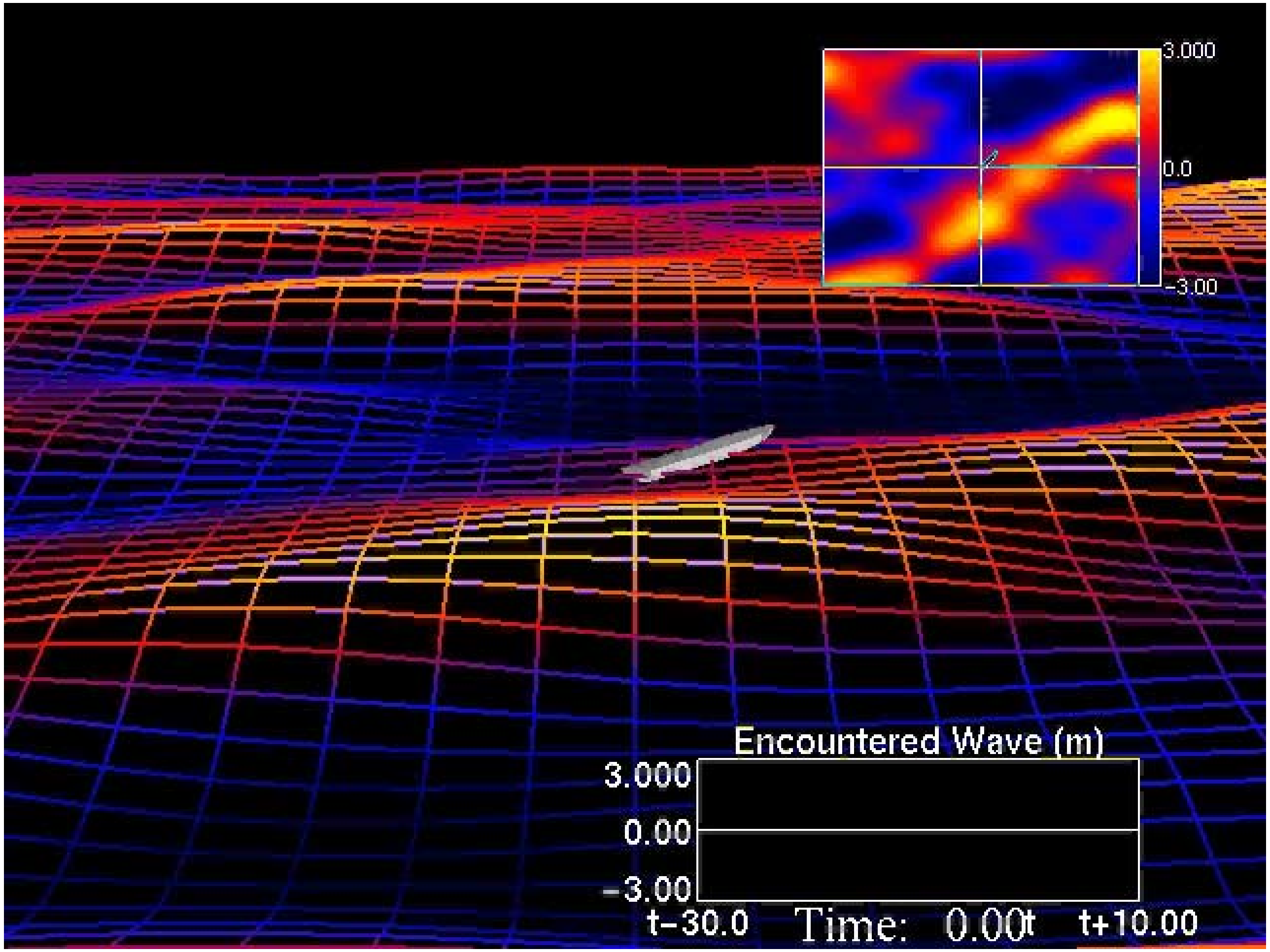

Demo 2: Helicopter Landing on Flight Deck

OBJECTIVE: To find window of opportunity (> 15 second duration of specified calm conditions) for helicopter landing/take-off.

DESCRIPTION:

- CG-47 ship in shortcrested seaway of sea state 6 with 10 knots forward speed (head seas).
- Time windows when operational criteria are above, below or near threshold limits are predicted (represented in a color scheme in the demo) .

Operation Indicator Chart Description

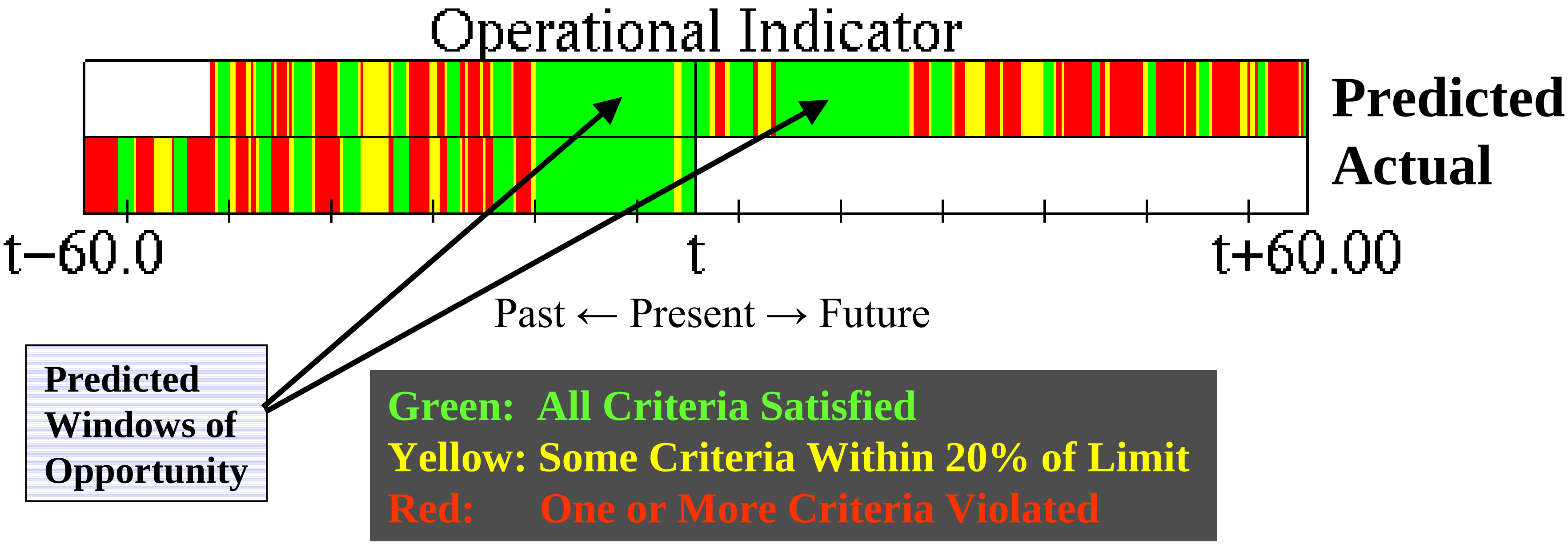

- Operational indicator chart scrolls from right to left in time where the center of the chart represents the current time.
- Actual/measured criteria is shown on the left side of the chart for comparison to the predicted criteria.
- Operational indicator gives operator a forecast of both the timing and duration of potential future windows of opportunities.
- **Flight Deck Operational Criteria for CG-47**

Criteria	Vertical Acceleration	Lateral Acceleration	Roll angle	Pitch angle
Launch/Recovery	0.2G	0.1G	2.5 deg	1.5 deg

Demo 2: Helicopter Landing on Flight Deck

Criteria Not Presently Satisfied | Criteria Presently Satisfied

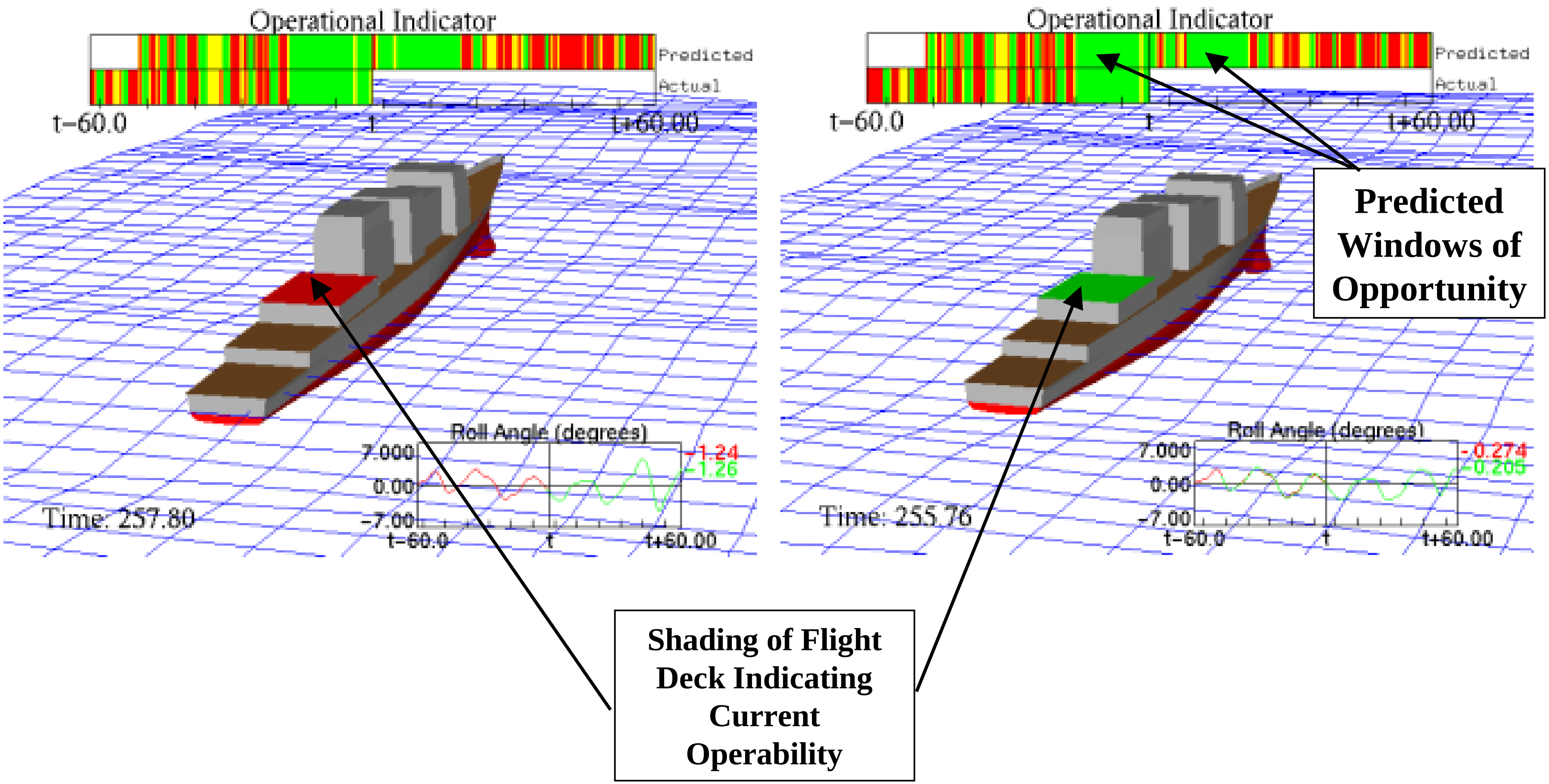

Demo 2: Helicopter Landing on Flight Deck

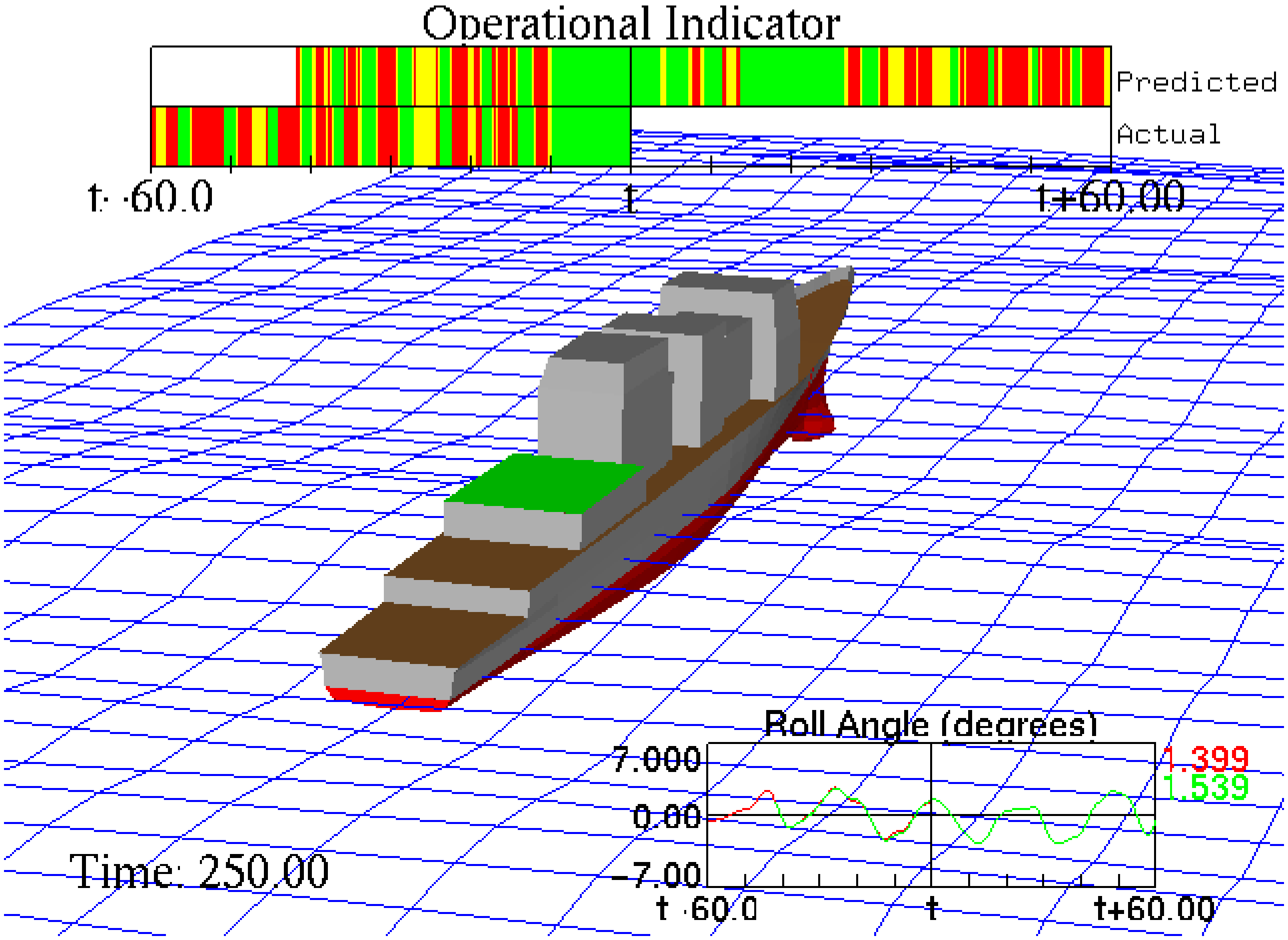

Conclusions

Technology Development for Severe Weather Automated/Assisted Ship Handling (SWASH)

- We have demonstrated the feasibility of SWASH by exploiting and integrating advances in the deterministic prediction of large-scale nonlinear wave-fields; large-amplitude ship motion simulations; and optimal control and estimation.
- Real-time realistic SWASH capability is likely in the near-term with further R&D concurrent with developments in sensor system technology and high-performance computing.
- A research plan is in place to achieve ~O(10) simulation vs. real time SWASH performance in the very near future, and ~O(1) time in the foreseeable future.

A Capability for Severe Weather Automated/Assisted Ship Handling (SWASH)

Dick K. P. Yue
Department of Ocean Engineering
MIT

END